



Dynamics of Ultrathin Vanadium Oxide Layers on Rh(111) and Rh(110) Surfaces During Catalytic Reactions

Bernhard von Boehn and Ronald Imbihl*

Institut für Physikalische Chemie und Elektrochemie, Leibniz Universität Hannover, Hannover, Germany

Over the past 35 years rate oscillations and chemical wave patterns have been extensively studied on metal surfaces, while little is known about the dynamics of catalytic oxide surfaces under reaction conditions. Here we report on the behavior of ultrathin V oxide layers epitaxially grown on Rh(111) and Rh(110) single crystal surfaces during catalytic methanol oxidation. We use photoemission electron microscopy and low-energy electron microscopy to study the surface dynamics in the 10^{-6} to 10^{-2} mbar range. On $\text{VO}_x/\text{Rh}(111)$ we find a ripening mechanism in which VO_x islands of macroscopic size move toward each other and coalesce under reaction conditions. A polymerization/depolymerization mechanism of VO_x that is sensitive to gradients in the oxygen coverage explains this behavior. The existence of a substructure in VO_x islands gives rise to an instability, in which a VO_x island shrinks and expands around a critical radius in an oscillatory manner. At 10^{-2} mbar the VO_x islands are no longer stable but they disintegrate, leading to turbulent redistribution dynamics of VO_x . On the more open and thermodynamically less stable Rh(110) surface the behavior of VO_x is much more complex than on Rh(111), as V can also populate subsurface sites. At low V coverage, one finds traveling interface pulses in the bistable range. A state-dependent anisotropy of the surface is presumably responsible for intriguing chemical wave patterns: wave fragments traveling along certain crystallographic directions, and coexisting different front geometries in the range of dynamic bistability. Annealing to 1000 K causes the formation of macroscopic VO_x islands. Under more reducing conditions dendritic growth of a VO_x overlayer is observed.

Keywords: vanadium oxide, chemical waves, methanol oxidation, heterogeneous catalysis, oxide redistribution

OPEN ACCESS

Edited by:

Marek Orlik,
University of Warsaw, Poland

Reviewed by:

Victor Bychkov,
Semenov Institute of Chemical
Physics (RAS), Russia
Rajkumar Kore,
University of Kansas, United States

*Correspondence:

Ronald Imbihl
imbihl@pci.uni-hannover.de

Specialty section:

This article was submitted to
Physical Chemistry and Chemical
Physics,
a section of the journal
Frontiers in Chemistry

Received: 05 May 2020

Accepted: 09 July 2020

Published: 21 August 2020

Citation:

von Boehn B and Imbihl R (2020)
Dynamics of Ultrathin Vanadium Oxide
Layers on Rh(111) and Rh(110)
Surfaces During Catalytic Reactions.
Front. Chem. 8:707.
doi: 10.3389/fchem.2020.00707

INTRODUCTION

Chemical waves and kinetic oscillations on catalytic surfaces have been studied starting from about 1980 with the vast majority focusing on reactions on metal surfaces (Ertl, 1991; Imbihl and Ertl, 1995; Imbihl, 2005). Low pressure ($p < 10^{-3}$ mbar) single crystal studies of catalytic CO oxidation and catalytic NO reduction on Pt, Rh, Pd and Ir catalysts yielded a plethora of different phenomena and they led to experimentally verified mechanisms. Despite the fact that the majority of the catalysts in chemical industry is based on oxidic materials, up to 2010 hardly any study of non-linear phenomena on oxidic catalysts existed. The reasons why metal catalyst were preferred against oxidic catalysts are easy to understand. Oxidic surfaces are structurally more complex, they are more difficult to prepare and surface analytical techniques based on electrons or ions are often of limited value due to beam damaging and electrical charging effects.

A concept to avoid these difficulties is based on the use of model systems in which ultrathin oxide layers are deposited on a metallic support. The main model system chosen here are submonolayer coverages of vanadium oxide deposited on a Rh(111) single crystal surface. Vanadium oxide based catalysts are widely applied in industrial catalysis, e. g., in partial oxidation reactions of hydrocarbons, in the selective catalytic reduction (SCR) in environmental catalysis, and in the production of sulfuric acid (Bond and Tahir, 1991). Important for the high catalytic activity is the ability of V to easily switch its oxidation state between +2 and +5. In most industrial applications, vanadium oxide catalysts are used in form of ultrathin layers, or as isolated clusters supported on an oxidic material of negligible catalytic activity. Of key importance is therefore knowledge about the dispersion of VO_x on a support material and redistribution dynamics under reaction conditions, which change the catalyst dispersion.

Besides the connection to “real catalysis,” the choice of the model system of supported submonolayer oxide films offers several advantages: (i) VO_x on Rh(111) exhibits a large number of ordered overlayers which have been exceedingly well characterized by surface analytical methods (Schoiswohl et al., 2004a,b; Surnev et al., 2013); for most of these overlayers structure models are available. (ii) Due to the electrically conducting support, electron-based analytical techniques can be applied. (iii) The system is strictly two-dimensional. Since V-oxides in their catalytically most active form are present either as isolated clusters or at monolayer coverages on a support material, studies of model catalysts with ultrathin layers of V-oxide are relevant to “real catalysis.”

The first aim of these studies was to see whether the spatially uniform distribution of the VO_x catalyst present after preparation is lifted under the influence of a catalytic reaction. Mostly the partial oxidation of methanol was chosen as reaction system, but also the $\text{H}_2 + \text{O}_2$ and other simple oxidation reactions were investigated. In fact, macroscopic stripe patterns and patterns of circular islands of VO_x developed under reaction conditions. The circular VO_x islands that developed exhibited a rather remarkable behavior. Two close-by islands moved toward each other and finally coalesced under reaction conditions (Hesse et al., 2015). Effectively, this leads to larger islands, similar to Ostwald ripening.

In order to see whether this type of behavior can be generalized, different reactions were investigated with VO_x on Rh(111) and, moreover, the Rh(111) substrate was exchanged against Rh(110) (von Boehn and Imbihl, 2018). The growth of VO_x on the more open and thermodynamically less stable surface Rh(110) surface is much more complex than on Rh(111) (von Boehn et al., 2017). In addition, this system had hardly been explored, so that no structure models were available. On the other hand, intriguing chemical wave patterns have been found in catalytic methanol oxidation on $\text{VO}_x/\text{Rh}(110)$, a behavior distinctly different from $\text{VO}_x/\text{Rh}(111)$ where only VO_x redistribution but no chemical wave patterns have been found. The results with both substrates, Rh(111) and Rh(110), are reviewed in this report.

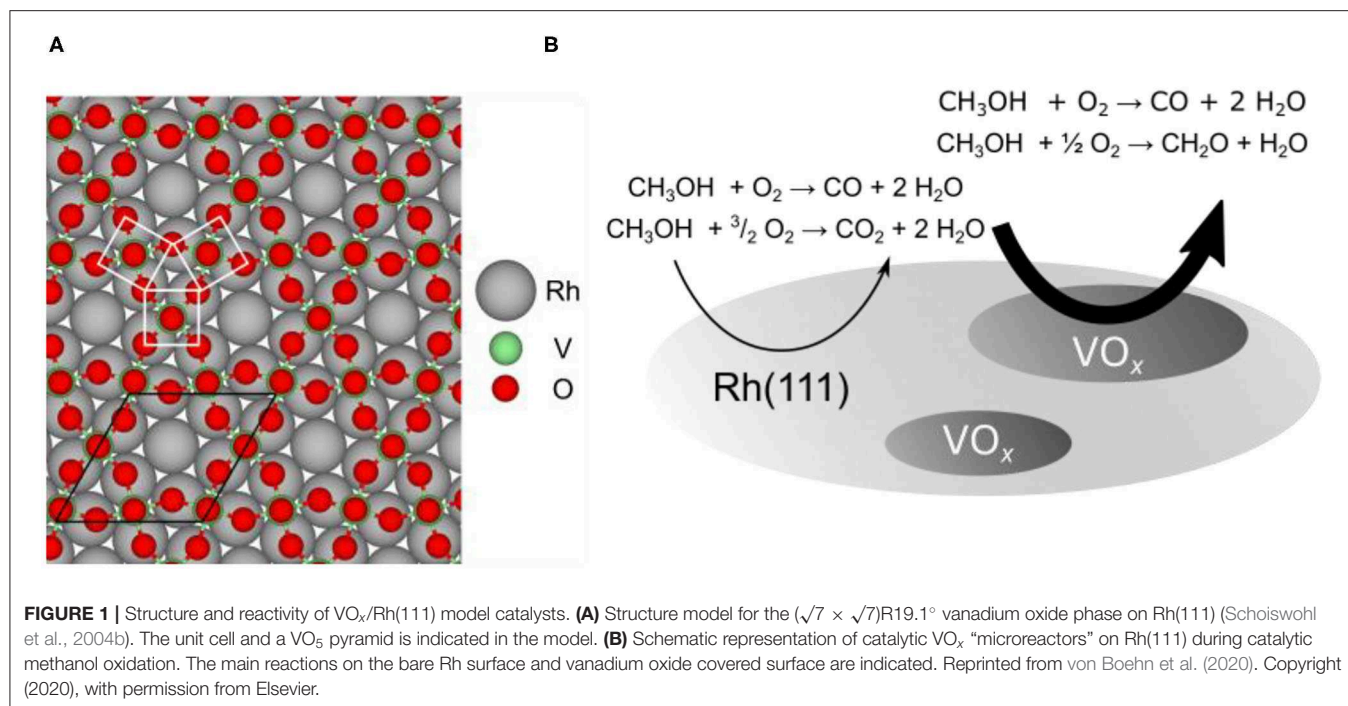
Model catalyst studies and “real catalysis” cannot be connected without addressing the so-called “pressure and materials gap” problem in heterogeneous catalysis (Schlögl, 2015). The main strategy to close the pressure gap is the use of *in situ* or operando techniques, because only then one obtains the structure/composition of the active catalyst that is required for establishing a structure-function relationship. The low-energy electron microscope (LEEM) that found extensive use in this study is a typical UHV instrument designed to be operated close to 10^{-10} mbar. In an effort to bridge at least a large part of the pressure gap, this LEEM instrument was modified, so that it could be operated up to 10^{-1} mbar (Franz et al., 2019). Applied to catalytic methanol oxidation on Rh(111)/ VO_x , this modified instrument revealed that at 10^{-2} mbar the VO_x islands are no longer stable but disintegrate, displaying turbulent behavior (von Boehn et al., 2020).

One aim of this review is to summarize the progress that has been achieved in the study of non-linear phenomena on catalytic oxide surfaces using the example of ultrathin supported V-oxide layers. A second goal is to demonstrate the significance of non-linear dynamics for catalytic research. Quite impressive wave patterns have been found in catalytic reactions on single crystalline metal surfaces, but asked about the significance for catalysis, many scientists would be very reluctant to concede any significance at all. Several examples presented in this review, like VO_x redistribution patterns connected to an activation of the catalyst or reaction-induced ripening of oxide islands, demonstrate very convincingly that a coherent understanding of the properties of a catalyst is not possible without taking dynamic phenomena into account.

REACTION DYNAMICS ON $\text{VO}_x/\text{Rh}(111)$ Choice of Model System and Methods of Investigation

As a model system for studying the redistribution of VO_x catalysts during several catalytic reactions we utilize submonolayer VO_x films on Rh(111). The system $\text{VO}_x/\text{Rh}(111)$ has been extremely well characterized in the monolayer and submonolayer coverage range (Schoiswohl et al., 2004b, 2005, 2006). Numerous ordered overlayers exist and structure models are available for many of them. All these structures can be described as network structures following the same building principle: VO_n ($n = 3-5$) units are connected by sharing oxygen atoms (Schoiswohl et al., 2004b). An example of such a two-dimensional network structure, the so-called $(\sqrt{7} \times \sqrt{7})\text{R}19.1^\circ$ structure, is shown in **Figure 1A**. The most abundant structural unit is a VO_5 pyramid with a V atom being above the center of a square base formed by four O atoms (V atom hidden in **Figure 1A** by an O-atom on top of it).

This system exhibits several advantages: (i) the system is strictly two-dimensional; (ii) VO_x is highly mobile on the flat Rh(111) surface, (iii) submonolayer VO_x films on Rh(111) have a high catalytic activity in many oxidation reactions, and (iv) charging problems are avoided thus allowing the use of electron-based surface analytical techniques. It should be added that the



properties of ultrathin V-oxide layers can be markedly different from the properties of V-oxide bulk compounds (Surnev et al., 2013).

In industrial heterogeneous catalysis, typically metallic catalysts are dispersed on an oxidic support, e.g., SiO_2 , Al_2O_3 , or TiO_2 . Here, oxides are deposited on a metallic support instead of a metal supported on an oxidic surface and, accordingly, the concept has been termed “inverse model catalyst” approach (Levin, 1987; Boffa et al., 1994; Surnev et al., 2013; Rodriguez et al., 2016). The concept of inverse model catalysts has several advantages. Charging problems with electron or ion based analysis techniques are avoided and the interface metal/oxide can be nicely studied. Moreover, the concept of inverse model catalysts has also been applied as a method to guide the development of novel catalysts (Zhang and Medlin, 2018).

In order to study the redistribution dynamics of VO_x spatially resolving techniques are required. In photoemission electron microscopy (PEEM) the sample surface is illuminated with UV light and the ejected photoelectrons are imaged (Rotermund, 1993). PEEM images primarily local work function variations with a lateral resolution of typically 0.1–1 μm . However, PEEM provides no or only indirect chemical and structural information. A technique that can provide the missing information is low-energy electron microscopy (LEEM) (Bauer, 2019) in its spectroscopic variant (SPELEEM) (Schmidt et al., 1998; Menteş et al., 2014). In LEEM, elastically backscattered, i.e., diffracted electrons in the energy range 0–200 eV are used to image the surface. Since the main contrast mechanism is diffraction contrast, LEEM is sensitive to structural changes of the surface, with the resolution being for most instruments around 10–15 nm, even though a resolution down to ~ 2 nm is possible (Wichtendahl et al., 1998). By putting in an aperture one

can obtain diffraction images of an area as small as 1 μm diameter (μLEED). Similarly, at synchrotrons providing the X-ray photons, one can use the instrument to obtain X-ray photoelectron spectroscopy from a 1 μm spot (μXPS). One can thus characterize the local surface structure as well as the local chemical composition. Since this instrument combines the spatial resolution of a microscope with the ability to perform local spectroscopy, this technique has also been termed “spectromicroscopy.”

Catalytic Activity and Dynamics of $\text{VO}_x/\text{Rh}(111)$

In industrial partial oxidation of methanol, the “formox” process (Franz et al., 2010), formaldehyde is the desired product. In methanol oxidation over $\text{VO}_x/\text{Rh}(111)$ three catalytic reactions have to be considered, as schematically shown in **Figure 1B**. On the bare $\text{Rh}(111)$ surface carbon dioxide, CO_2 , is formed as product of the total oxidation:



Besides total oxidation, also carbon monoxide, CO , and formaldehyde, CH_2O , are formed as products of the partial oxidation of methanol according to:



While CO is produced on both surfaces, bare $\text{Rh}(111)$ and VO_x covered $\text{Rh}(111)$, the formation of formaldehyde is restricted to the VO_x covered parts of the surface (Hesse et al., 2015).

The mechanism of methanol oxidation over oxide-supported V-oxide has been clarified in a number of quantum chemical studies (Döbler et al., 2005; Göbke et al., 2009; Kropp et al., 2014). More specifically, vanadyl groups (V=O) were shown to play an essential role in the reaction mechanism of formaldehyde formation from methanol over VO_x catalysts. Such vanadyl groups were found in some of the two-dimensional network structures of VO_x on Rh(111), for example in the ($\sqrt{7} \times \sqrt{7}$)R19.1° shown in **Figure 1A** (Schoiswohl et al., 2004b). In general, a mechanistic explanation of partial oxidation reactions over oxidic surfaces is often based on a two-step model originally proposed by Mars and van Krevelen (Frank et al., 2009; Carrero et al., 2014). First lattice oxygen from the oxidic catalyst is transferred to the reactant, which is oxidized. In a second step, the reduced oxide catalyst is reoxidized.

We investigate whether the initial homogeneous distribution of V-oxide is maintained during a catalytic reaction. The starting point of every VO_x redistribution experiment is a Rh(111) surface homogeneously, on a μm length scale, covered with a submonolayer quantity of VO_x. It should be stressed that if the surface is homogeneous on a macroscopic scale (> 1 μm), on a microscopic scale it might be heterogeneous. Such a surface is exposed to a gas atmosphere consisting of methanol and oxygen in the 10⁻⁴ mbar range and heated to 1030 K (0.2–0.5 K/s), starting from 300 K. At around 770–820 K the initially homogeneous surface state is lifted and a regular stripe pattern develops, as shown in a series of PEEM images (stage I) in the top panel of **Figure 2**. In PEEM a low work function (WF) surface is imaged as bright area, high WF regions as dark area. Adsorbed oxygen, due to the high dipole moment of the adsorbate complex O-Rh, appears dark in PEEM, but so does V-oxide (if V is in a V⁴⁺ or V⁵⁺ state). Therefore, with PEEM alone, the interpretation of the images is not clear. Subsequent μXPS measurements (below) showed that the dark islands in **Figure 2** represent V-oxide covered area, whereas the surrounding area is largely V-oxide free (Lovis et al., 2011; Hesse et al., 2015).

Remarkably, the condensation of the highly dispersed VO_x into a stripe pattern is accompanied by a drastic increase of the formaldehyde production (bottom panel of **Figure 2**). As the temperature is further increased the stripe pattern coarsens up to roughly 980 K (stage II), followed by a transformation into a spot pattern of circular, several tens to hundreds μm wide vanadium oxide islands (stage III).

The formation of a VO_x stripe pattern followed by a transition into a spot pattern of VO_x islands is observed in a number of different chemical reactions on VO_x/Rh(111), including the oxidation of H₂, CO and ammonia (Lovis and Imbihl, 2011; von Boehn et al., 2016). **Figure 3A** shows the coarsening of a VO_x stripe pattern under constant reaction condition on VO_x/Rh(111) during the H₂ + O₂ reaction at 773 K. The pattern is the result of V and O forming a dense VO_x coadsorbate phase. The surrounding bright surface is bare Rh(111) surface. The initially thin, dark stripes in the first PEEM image of **Figure 3A** increase their width, and after about 1000 s further progress is happening rather slowly. However, the coarsening still continues and we cannot deduce a value to which the curve asymptotically approaches.

This behavior is also reflected in a plot of the wavenumber $k = 1/\lambda$ of the stripe pattern vs. time plot, as demonstrated in **Figure 3B**. The coarsening process obeys a power law $k(t) \propto t^{-\beta}$ with $\beta = 0.23 \pm 0.03$, as shown in **Figure 3C**. For the dependence of the wavenumber k on the pressure, a power law $k(p) \propto p^\alpha$ was experimentally determined with $\alpha = 0.33 \pm 0.05$. The wavenumber k increases with increasing pressure in the pressure range between 10⁻⁶ and 10⁻⁴ mbar.

For explaining pattern formation in this system, the concept of reactive phase separation seemed to be applicable. Attractive or repulsive interactions between adsorbed particles on a surface can result in the condensation into a dense phase. Thermodynamically, an island of infinite size should finally result but, coupled to a chemical reaction, a finite size is selected. On a potassium promoted Rh(110) surface reactive phase separation was observed during the H₂ + O₂ reaction (De Decker et al., 2004). Later on, reactive phase separation was also demonstrated on Pd and Au alloyed Rh(110) surfaces in the H₂ + O₂ reaction (Locatelli et al., 2005, 2006). The prerequisites for reactive phase separation to occur are not very restrictive, since only a sufficient mobility of the components and different chemical affinity between the reacting adsorbates are required. What does not fit into the concept of reactive phase separation in the present case is that the coarsening does not approach a finite value. A control experiment in which V-oxide on Rh(111) was annealed in O₂ only, revealed that also in this case VO_x islands of macroscopic size are formed (von Boehn et al., 2016). The condensation of VO_x into stripes and circular islands under reaction conditions therefore appears to be driven by thermodynamics.

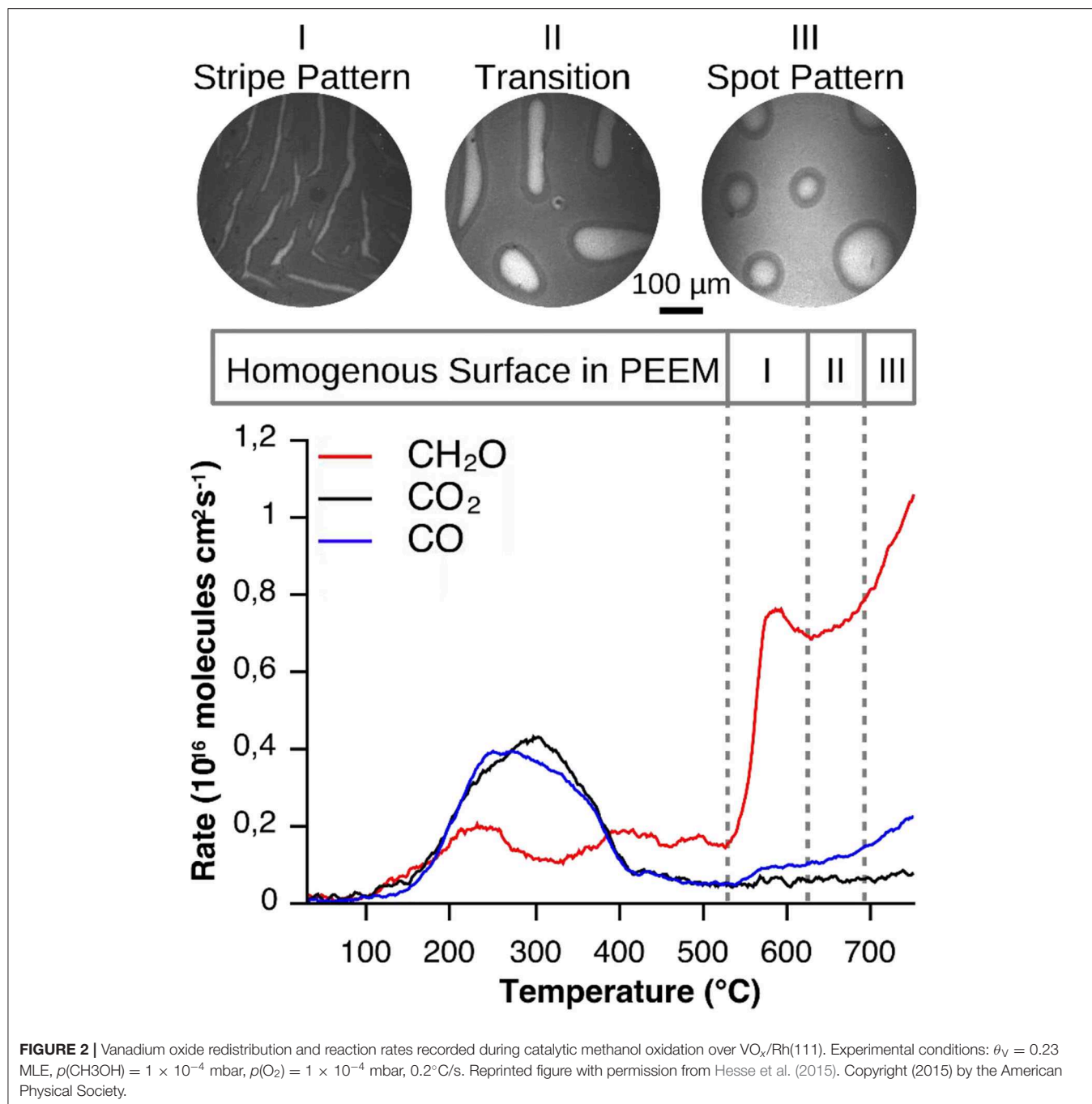
Under strongly reducing conditions, the reduction of VO_x can proceed until metallic V is formed, which forms surface and subsurface alloys with Rh(111) at sufficiently high temperature (1023 K) in vacuum (Piš et al., 2012). However, even low oxygen pressures in the 10⁻⁷–10⁻⁸ mbar range suffice to stabilize V as an oxide on the surface (Schoiswohl et al., 2005). Thus, under the conditions of catalytic reactions V is localized on the Rh(111) surface and no V/Rh surface or subsurface alloy is formed. This simplifies the analysis considerably.

VO_x Islands Coalescence

Experimental Observations

In the last stage of the self-organization process, stage III in **Figure 2**, circular tens to hundreds μm wide VO_x islands are distributed on the Rh(111) surface. Remarkably, if two V-oxide islands are within a critical distance of the order of 100 μm, they move toward each other and coalesce under reaction conditions. The series of PEEM images in **Figure 4A** shows the coalescence of two neighboring VO_x islands during catalytic methanol oxidation in the 10⁻⁴ mbar range. As the inter-island distance decreases, the movement of the two islands accelerates until they finally merge, as shown in **Figure 4B**. Interestingly, this coalescence proceeds exclusively under the conditions of an ongoing catalytic reaction. Stopping the supply of one of the two reactants, oxygen and methanol, instantly freezes the island movement.

One also notes that above a critical size the islands in **Figure 4A** exhibit a substructure consisting of an inner bright



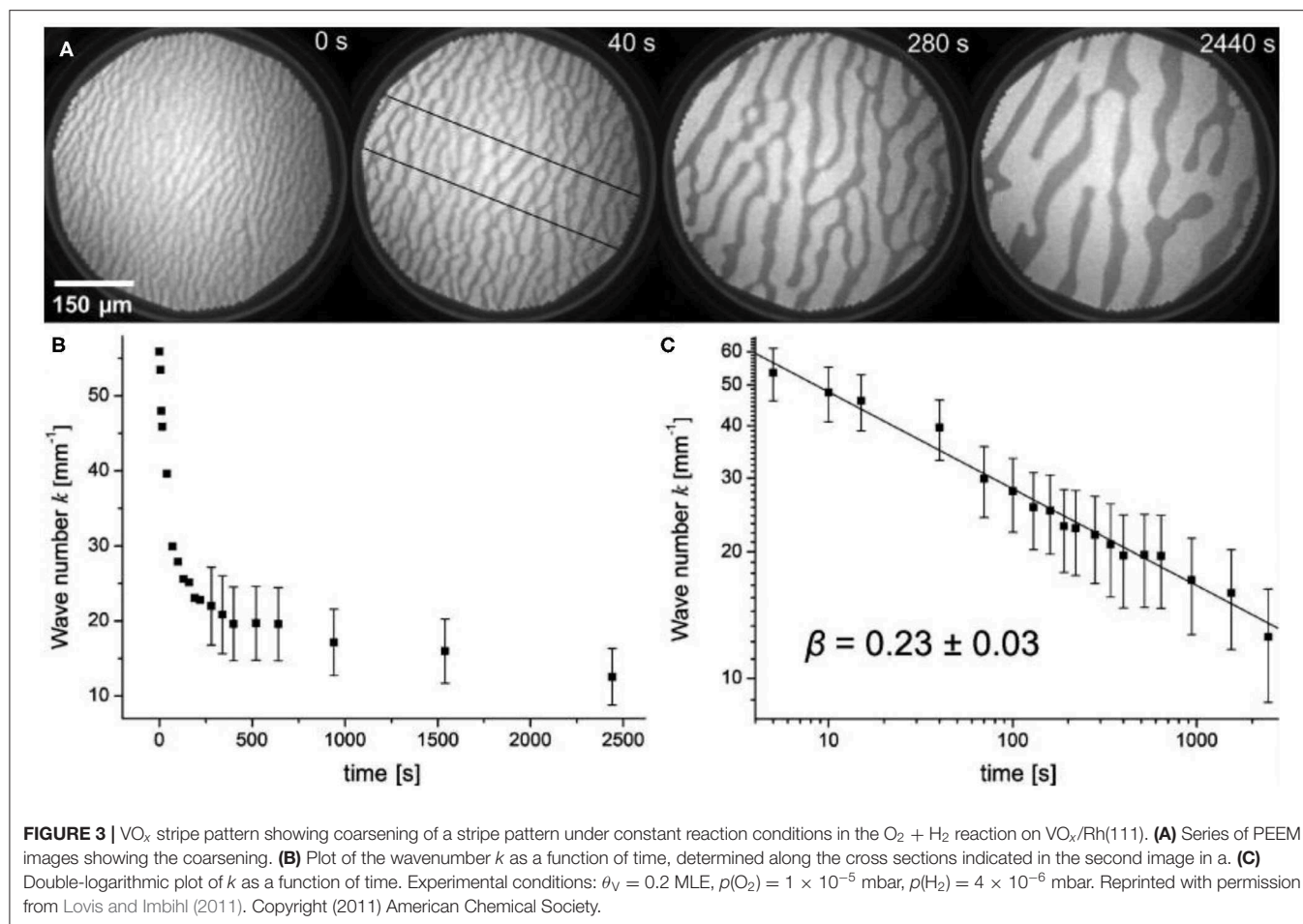
core, surrounded by an outer dark ring. This substructure is the result of V in the core being in a more reduced state than in the outer ring. This will be described below in more detail.

The island coalescence leads to an island ripening as in classical Ostwald ripening, where large islands grow at the expense of smaller ones. However, whereas Ostwald ripening occurs close to thermodynamic equilibrium, ripening via island coalescence takes place only under conditions far from equilibrium. The island coalescence mechanism is similar to Smoluchowski ripening, where island coarsening proceeds via collision of larger adatom aggregates, clusters or islands

that diffuse randomly on the surface (Thiel et al., 2009). Smoluchowski ripening, however, does not require a chemical reaction, and the diffusing islands and clusters comprise only a small number of atoms. The unusual behavior seen here is the directed movement of large macroscopic islands that would normally require the existence of a macroscopic force.

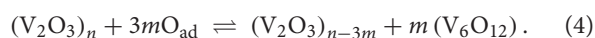
The Polymerization/Depolymerisation Mechanism

For understanding the peculiar behavior of VO_x islands under reaction conditions, one has to take a closer look at the surface chemistry of V-oxides on Rh(111). Molecular oxygen has a



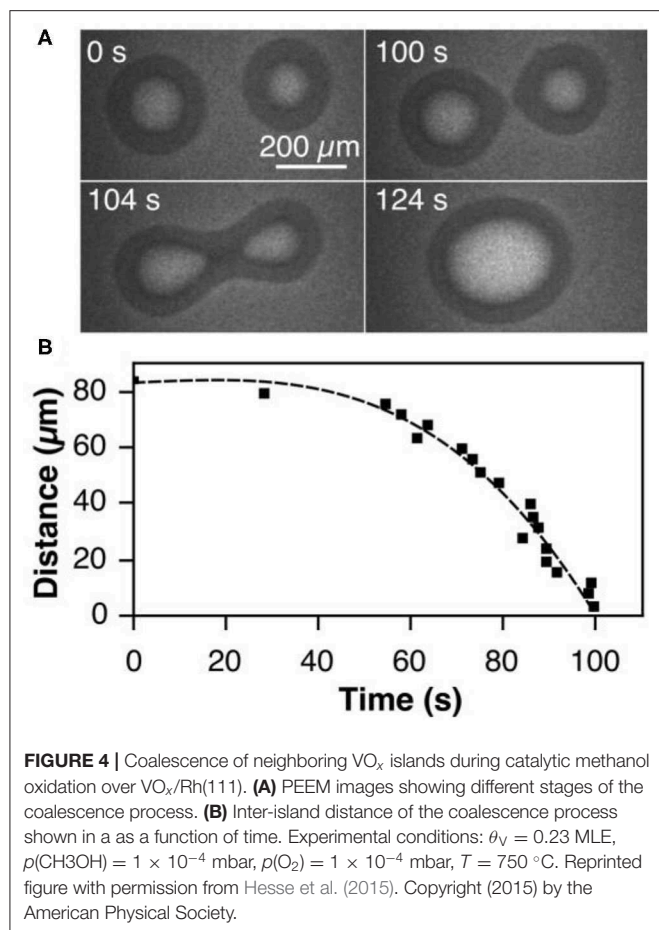
low sticking coefficient on the VO_x covered Rh(111) surface, but it can readily adsorb on the metallic Rh(111) surface. As a consequence, O_{ad} is diffusively transported from the surrounding metallic Rh(111) surface toward the VO_x islands, where formaldehyde production almost exclusively takes place and where the oxygen is consumed. Due to the high catalytic activity of VO_x, the macroscopic V-oxide islands can therefore be considered as “catalytic microreactors” which consume oxygen for the oxidation reaction, and thus act as sinks for adsorbed oxygen. The diffusive supply of O_{ad} to the VO_x islands generates gradients in the oxygen coverage around the V-oxide islands.

Observations with scanning tunneling microscopy on VO_x islands on Rh(111) demonstrated that at 380 K, isolated V₆O₁₂ clusters can detach from a large VO_x island (Schoiswohl et al., 2004a). If the cluster is part of a network structure in a VO_x island, additional oxygen is needed to detach the clusters, because in the network the individual units are connected by sharing corner oxygen atoms. If we take a V₂O₃ composition for the large VO_x islands, we can formulate a polymerization/depolymerisation (PD) or association/dissociation equilibrium:



This is a chemical equilibrium that is controlled by the oxygen coverage. A high oxygen coverage favors the dissociation of the large island into small clusters; conversely, a low oxygen coverage shifts the equilibrium toward aggregation of the clusters. The oxygen gradients developing under reaction conditions around VO_x islands and the PD equilibrium suffice to explain the island coalescence as schematically depicted in **Figure 5**. In region I in **Figure 5A**, the oxygen coverage is considerably lower than in region II, since two neighboring VO_x islands compete as sinks for adsorbed oxygen. According to the PD equilibrium of Equation (4), a high oxygen coverage in regions II favors depolymerization of the VO_x islands into small V₆O₁₂ clusters. Since the low oxygen coverage in region I shifts the equilibrium to the polymerization side, the small V₆O₁₂ clusters become attached again to the VO_x islands, but now on the opposite side from where they became detached. The net result is that the two neighboring islands move toward each other.

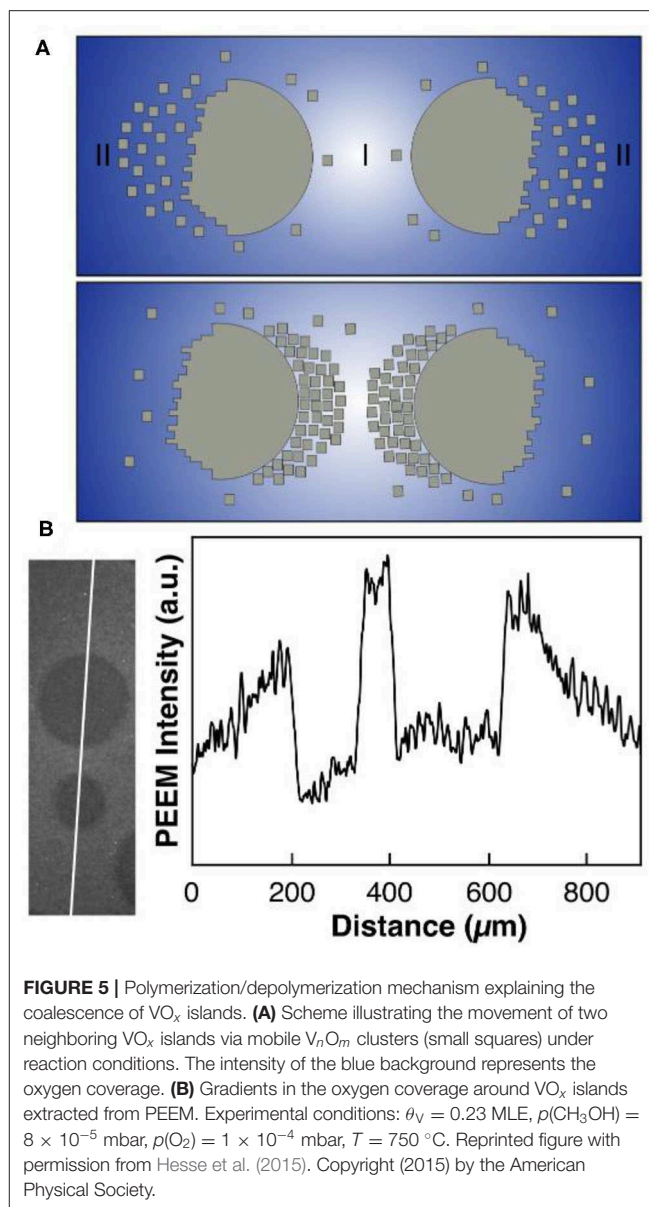
An essential requirement of this mechanism is that the V₆O₁₂ clusters and adsorbed oxygen exhibit a sufficiently high diffusivity. Both is the case as shown by experimental data (Barth, 2000; Mavrikakis et al., 2002; Schoiswohl et al., 2004a). Experiments in which VO_x islands pinned to defects “evaporated” demonstrated the existence of small mobile VO_x clusters, because desorption of VO_x into the gas phase can be



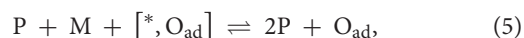
excluded (Hesse et al., 2015). The diffusivity of atomic oxygen on Rh(111) fixes the length scale of the oxygen gradients, and this value of roughly 100 μm is equal the critical distance below which two neighboring islands start to feel the attraction of the other island. The existence of oxygen gradients around VO_x islands shows up in brightness variations in PEEM (**Figure 5B**) and, more directly, in concentration profiles recorded with μXPS (below). The mechanism sketched above explains why island movement only occurs under reaction conditions since, without reaction, the oxygen gradients immediately vanish. Clearly, no macroscopic force is needed to move the islands because the movement takes place via the transport of small V_nO_m clusters.

Modeling VO_x Islands Coalescence

The island coalescence in the system $\text{CH}_3\text{OH} + \text{O}_2/\text{VO}_x/\text{Rh}(111)$ has been reproduced with a skeleton reaction-diffusion model (De Decker et al., 2019). This model considers a highly simplified reaction mechanism, but takes into account the PD mechanism including the adsorption of oxygen and the existence of energetic interactions between the adparticles. Strong lateral interactions between the VO_x polymers are evidenced by the nearly circular shape of the VO_x islands, which indicates a strong internal cohesion.

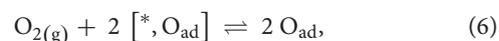


The small V_nO_m clusters through which VO_x mass transport is mediated are represented as “monomers” M in the model, extended V-oxide areas are described as “polymer” P. The polymerization / depolymerization equilibrium in Equation (4) can then be written as:



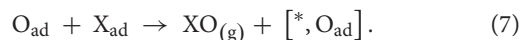
with $[* , \text{O}_{\text{ad}}]$ representing an unoccupied adsorption site for O_{ad} .

Adsorbed oxygen is formed by dissociative adsorption from the gas phase,



and through the condensation process of monomers described in Equation (5). Oxygen is removed through desorption and

through reaction with a molecule X (e.g., methanol) according to



As outlined above, this reaction proceeds with a considerable higher rate on the vanadium oxide islands (catalytic “microreactors”) than on the bare metal surface. The different catalytic activity is taken into account via the rate constant of the catalytic reaction, which is a function of the local polymer coverage θ_{P} .

The surface diffusion of atomic oxygen (D_{O}), of the monomer M (D_{M}), and of the polymer P (D_{P}) are taken into account with $D_{\text{O}} > D_{\text{M}} \gg D_{\text{P}}$. Due to the existence of energetic interactions between adsorbed particles and due to site exclusion, diffusion is non-Fickian.

Numerical integration of the reaction-diffusion-equations shows that a region of bistability exists in which the homogeneous distribution of VO_x decays spontaneously into a P-rich and a P-poor phase in a quasi-spinodal decomposition. The domain size does not approach an asymptotic value in time but continuously increases as experimentally observed in the $\text{H}_2 + \text{O}_2$ reaction on $\text{VO}_x/\text{Rh}(111)$ (Figure 3).

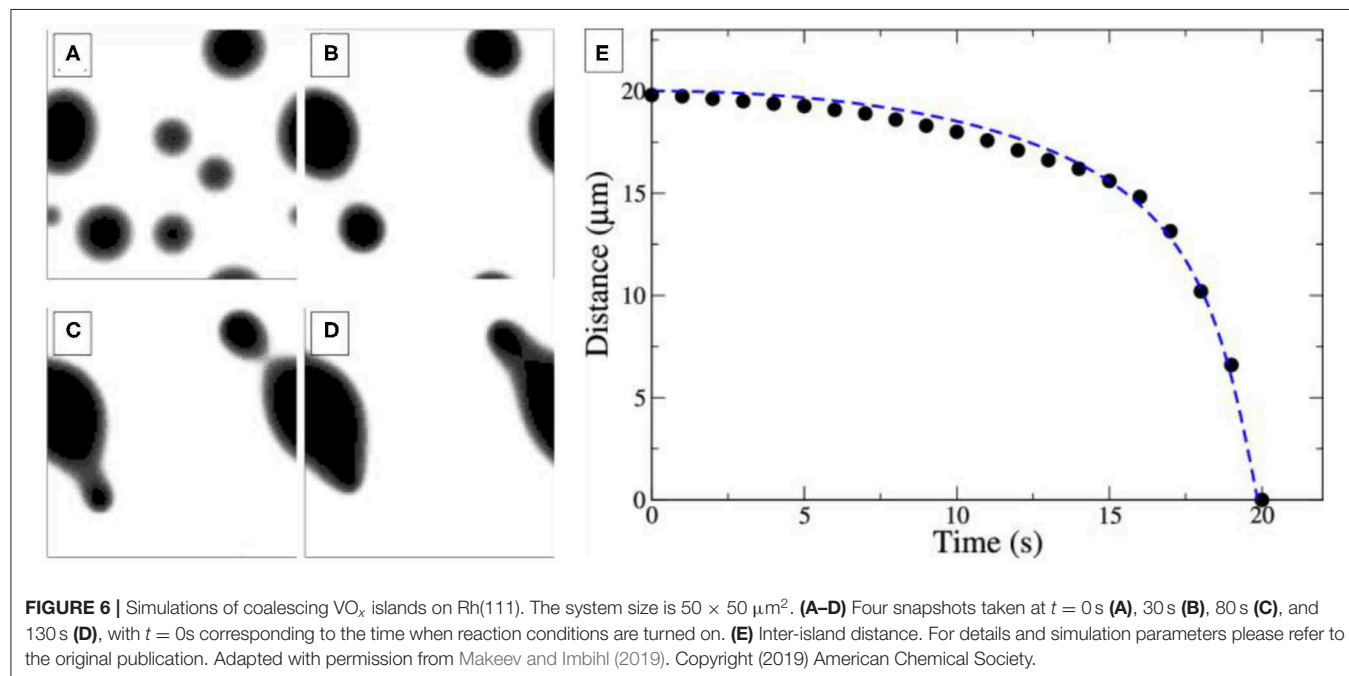
As one increases both, the reaction rate and the O_2 adsorption rate, which in experiments corresponds to elevated temperature and pressure, one observes the behavior depicted in Figure 6. Close-by islands move toward each other and coalesce. Directly after coalescence the islands are deformed, but the circular shape is restored within a short time. The distance between the two coalescing islands plotted vs. time in Figure 6E displays qualitatively the same behavior as the experimental dependence in Figure 4B. A close look at the concentration profiles corroborates the mechanistic interpretation given above. It is the sensitivity of the PD

equilibrium to gradients in the oxygen coverage that leads to the transport of VO_x and causes the movement of the VO_x islands toward each other.

The reaction-diffusion equations allow even to derive an equation of motion for the islands using Newtonian mechanics. Numerical integration of this Newtonian law reproduces well the trajectories obtained from simulations of the full model, as demonstrated in Figure 6E (dashed blue line).

VO_x Island Substructure

The PEEM images in Figures 2, 4A show that the VO_x islands exhibit a substructure consisting of a bright core and a dark outer ring. The missing chemical information is provided by μXPS , allowing also for quantification of the surface coverages. After preparation of a VO_x island in the 10^{-4} mbar range, local XP spectra were taken under reaction conditions in the 10^{-6} mbar range across the island (Hesse et al., 2015). One thus obtains a cross section through the island displayed in Figure 7A. A shift of the V 2p core level toward higher binding energy (BE) in Figure 7B indicates that vanadium in the outer ring is in a more oxidized state than in the core region. A comparison of the V 2p BEs from the spectra with the BEs from V-oxide bulk compounds (neglecting possible effects from the monolayer thickness), shows that in the center of the island $\text{V}^{3+}/\text{V}^{4+}$ species prevail, whereas in the outer ring V is mainly in the oxidation state +4/+5. This finding agrees with the picture of VO_x islands as “microreactors,” because with oxygen being transported diffusively from the island boundary, naturally an oxygen concentration gradient will arise inside the island caused by oxygen consumption in the reaction. Above a critical island size, the supply of oxygen will not be high enough to maintain a high oxidation state of vanadium in the core region of the island, and a reduction through reaction with methanol will occur.



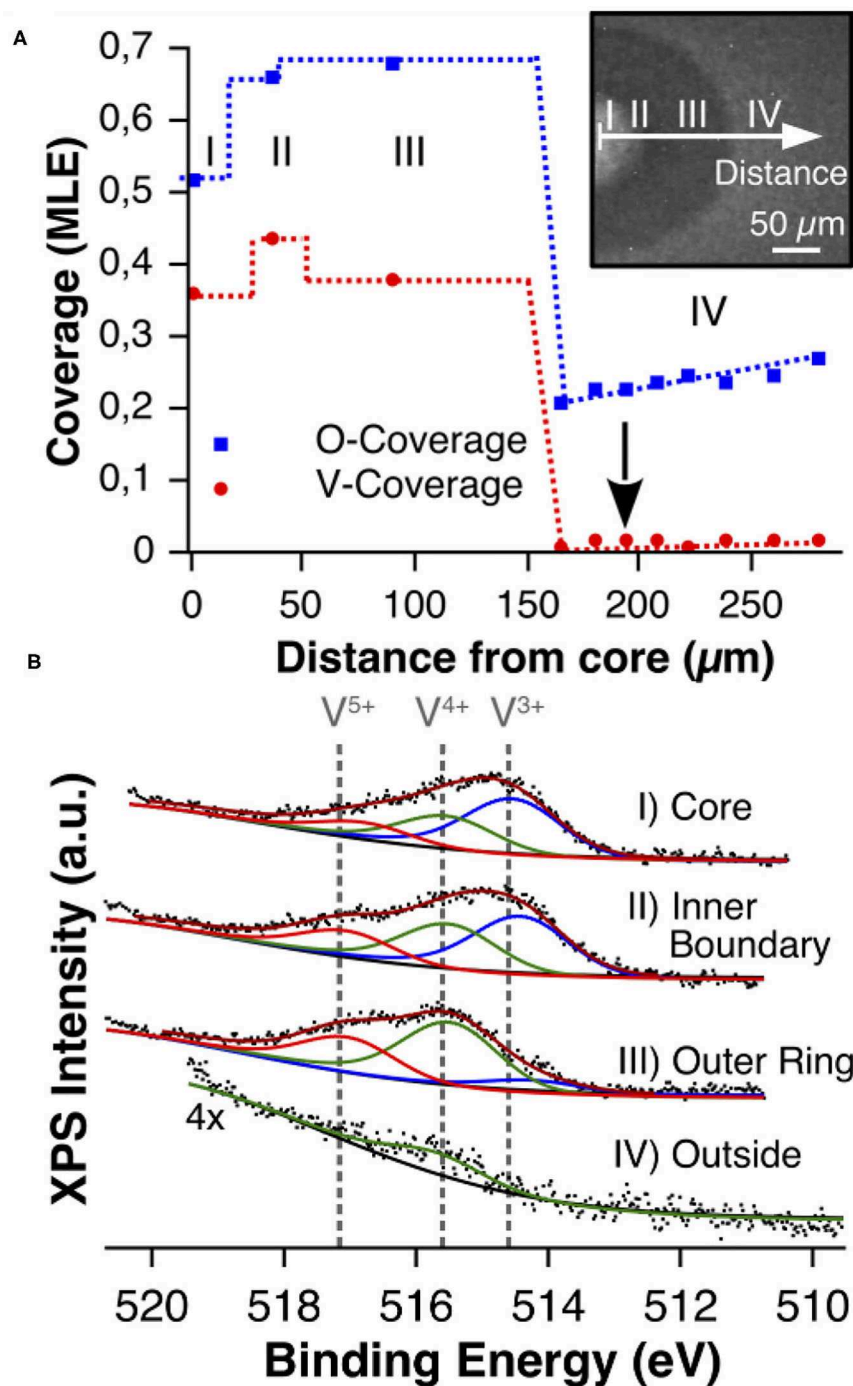


FIGURE 7 | Chemical characterization of a VO_x island with XPS during catalytic methanol oxidation over $\text{VO}_x/\text{Rh}(111)$. **(A)** V and O coverage profile recorded under reaction conditions in the 10^{-6} mbar range. The position $0\ \mu\text{m}$ refers to the island center. **(B)** V $2p_{3/2}$ core level spectra recorded with μXPS on various positions inside and outside (arrow) the VO_x island. Reprinted figure with permission from Hesse et al. (2015). Copyright (2015) by the American Physical Society.

As expected from the picture of the “microreactor,” the oxygen coverage is high outside the VO_x islands and a gradient is clearly visible from a high oxygen coverage far away from the island toward a lower coverage at the boundary. Outside the VO_x islands, only a small amount of vanadium oxide is detected,

representing the mobile V_nO_m clusters through which the island coalescence proceeds.

Besides the island radius, the existence of a substructure also depends on the reaction conditions. A high amount of methanol favors the formation of a reduced core. One should add that VO_x

islands can be prepared with a substructure involving a number of clearly distinguishable phases (von Boehn, 2020). The effect of the substructure on the dynamics of an island is demonstrated in the following.

Oscillating VO_x Islands

Two subsequent LEEM images showing two stages in the oscillatory behavior of a circular VO_x island during catalytic methanol oxidation are shown in **Figure 8A**. Reaction conditions are in the 10⁻⁴ mbar range. Different from PEEM, whose main contrast mechanism is based on local work function variations, LEEM is a structure sensitive microscopy technique, which additionally allows for laterally resolved LEED measurements. The brightness levels in LEEM are not related to the brightness levels in PEEM, since the contrast mechanisms are different. In the LEEM images one observes a core region, a dark outer ring and, in addition to the substructure visible in PEEM, a band separating core and outer ring.

Surprisingly, despite constant parameters, the island exhibits an oscillatory cycle in which the island undergoes a periodic expansion and contraction, simultaneously with periodic brightness variations in the core of the island (von Boehn et al., 2020). The transformations from a bright core to a dark core and vice versa take place via reaction fronts nucleating at the boundary of the core. The periodic LEEM intensity changes of the different VO_x phases as well as the changes in the positions of the three interfaces are displayed in **Figure 8B**. Practically only the outer ring changes its size and the size oscillations display a strict phase relationship with the periodic intensity changes in the core that we can associate with a reduction and oxidation, respectively. A remarkable fact is that in this “breathing” of the island a considerable mass transport of VO_x has to occur to accomplish the variations in island size.

With *in situ* μLEED ordered VO_x overlayers could be identified in the breathing island: a ($\sqrt{7} \times \sqrt{7}$)R19.1° structure for the outer ring and a ($\sqrt{3} \times \sqrt{3}$)-Moiré structure for the core region (von Boehn et al., 2020). To understand the occurrence of different phases in the VO_x island is quite straightforward using the picture of the VO_x islands as catalytic micro-reactors. Since inside the oxide islands a gradient in the chemical potential of oxygen exists, a cross section through a VO_x island corresponds to a cross section through a phase diagram of VO_x on Rh(111), with the chemical potentials of oxygen and vanadium as intensive variables.

Such a phase diagram has been calculated with density functional theory (DFT) for the system VO_x/Rh(111) and the result is displayed in **Figure 9A**. The ($\sqrt{7} \times \sqrt{7}$)R19.1° structure of the highly oxidized ring is present, but the ($\sqrt{3} \times \sqrt{3}$)-Moiré structure of the core does not occur in the phase diagram. This ($\sqrt{3} \times \sqrt{3}$)-Moiré structure has not been reported in the literature and no structure model exists. Probably, this structure does not represent an equilibrium structure and therefore does not show up in a phase diagram of VO_x/Rh(111). Since V in the reduced core is present as V³⁺, a (2 × 2) V₂O₃ structure with a V coverage of 0.5 MLE is predicted from the phase diagram for the reduced island core.

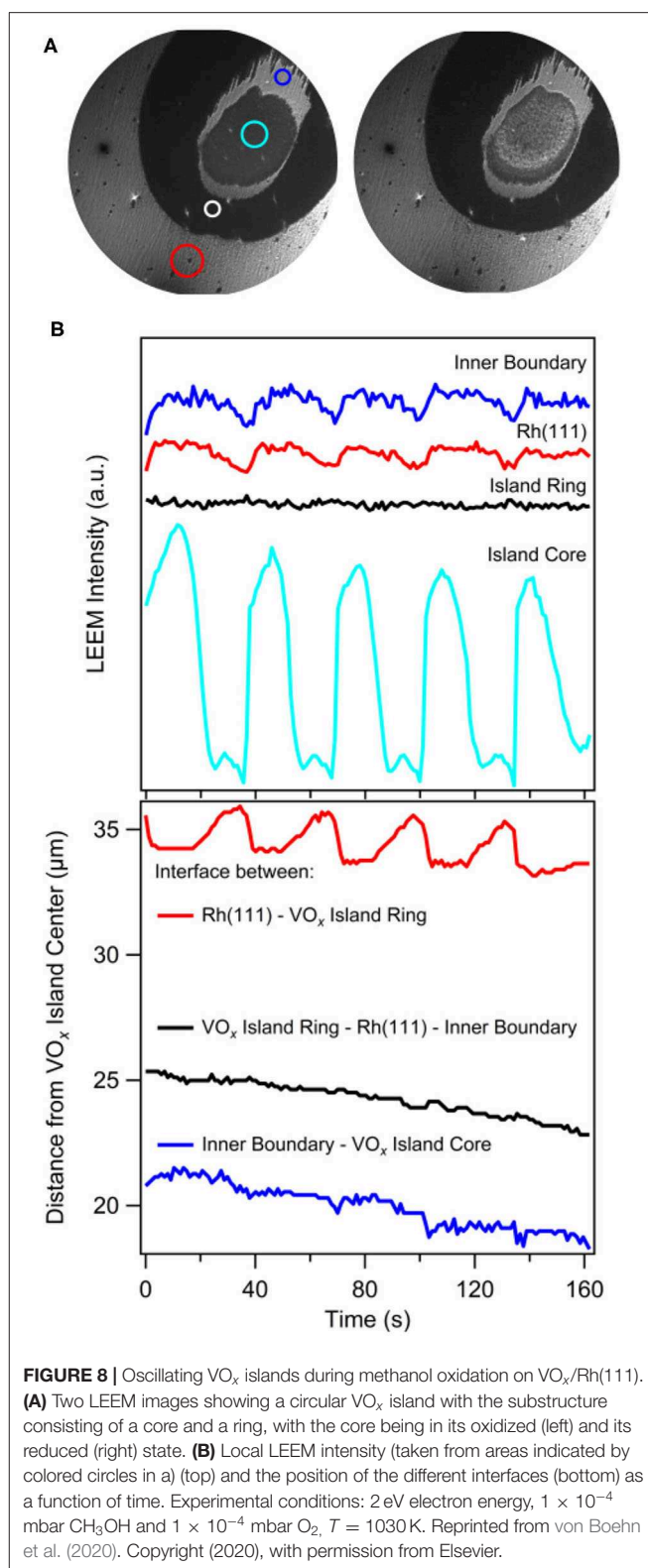
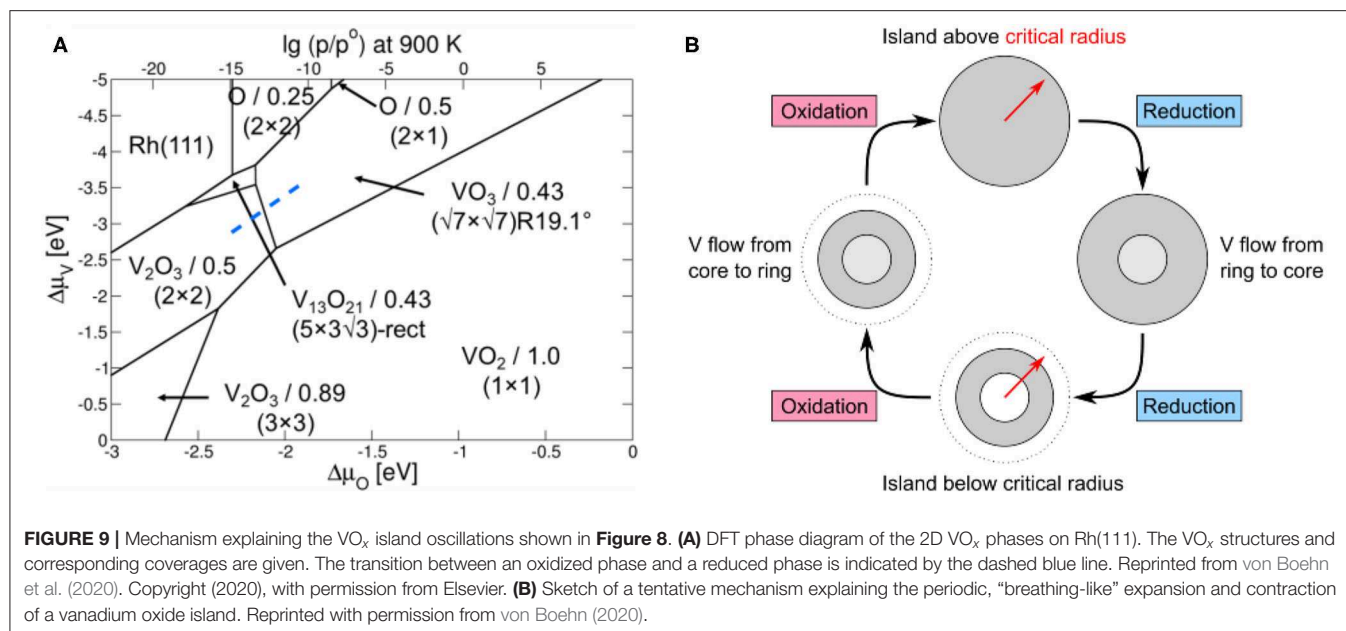


FIGURE 8 | Oscillating VO_x islands during methanol oxidation on VO_x/Rh(111). **(A)** Two LEEM images showing a circular VO_x island with the substructure consisting of a core and a ring, with the core being in its oxidized (left) and its reduced (right) state. **(B)** Local LEEM intensity (taken from areas indicated by colored circles in a) (top) and the position of the different interfaces (bottom) as a function of time. Experimental conditions: 2 eV electron energy, 1 × 10⁻⁴ mbar CH₃OH and 1 × 10⁻⁴ mbar O₂, T = 1030 K. Reprinted from von Boehn et al. (2020). Copyright (2020), with permission from Elsevier.

The phase diagram reveals that the reduced VO_x phases have a higher V density than oxidized VO_x phases, a relation that also became apparent from the experimentally determined V



and O coverages for the different 2D- VO_x phases on Rh(111) (Schoiswohl et al., 2004b, 2005; von Boehn et al., 2020). For explaining the size oscillation, only one other relation is required. Since periodic oxidation/reduction fronts transform the core of the island, the island size has to be in the vicinity of the critical radius for existence of a reduced core. With these two ingredients, *i*) different V densities for reduced and oxidized VO_x phase, and *ii*) the island size being around the critical radius for the formation of a reduced core in VO_x , we can set up a mechanism for the size oscillations. We assume that in the oxidation/reduction of the island core, we move along the blue dashed line in the PD of Figure 9A.

A Schematic Representation of the Proposed Mechanism is Shown in Figure 9B:

- Initially, the island is above the critical island radius, but the core is still in a completely oxidized state. Due to the long distance over which O_{ad} has to diffuse, not enough oxygen reaches the core, and a reduction of the core sets in. Since the reduced VO_x phase has a higher V density, extra V atoms are needed. They are taken from the outer ring and are transported from there to the island center.
- The transport of V atoms to the island core results in a shrinking of the oxidized ring, which eventually falls below the critical radius.
- Due to the shorter distance O atoms now have to cover, the O coverage in the island core increases, finally triggering the transformation of the core back into the oxidized state.
- Due to the lower V density in the oxidized state, extra V atoms are expelled from the core. They migrate back to the outer ring, which grows thus closing the oscillatory cycle.

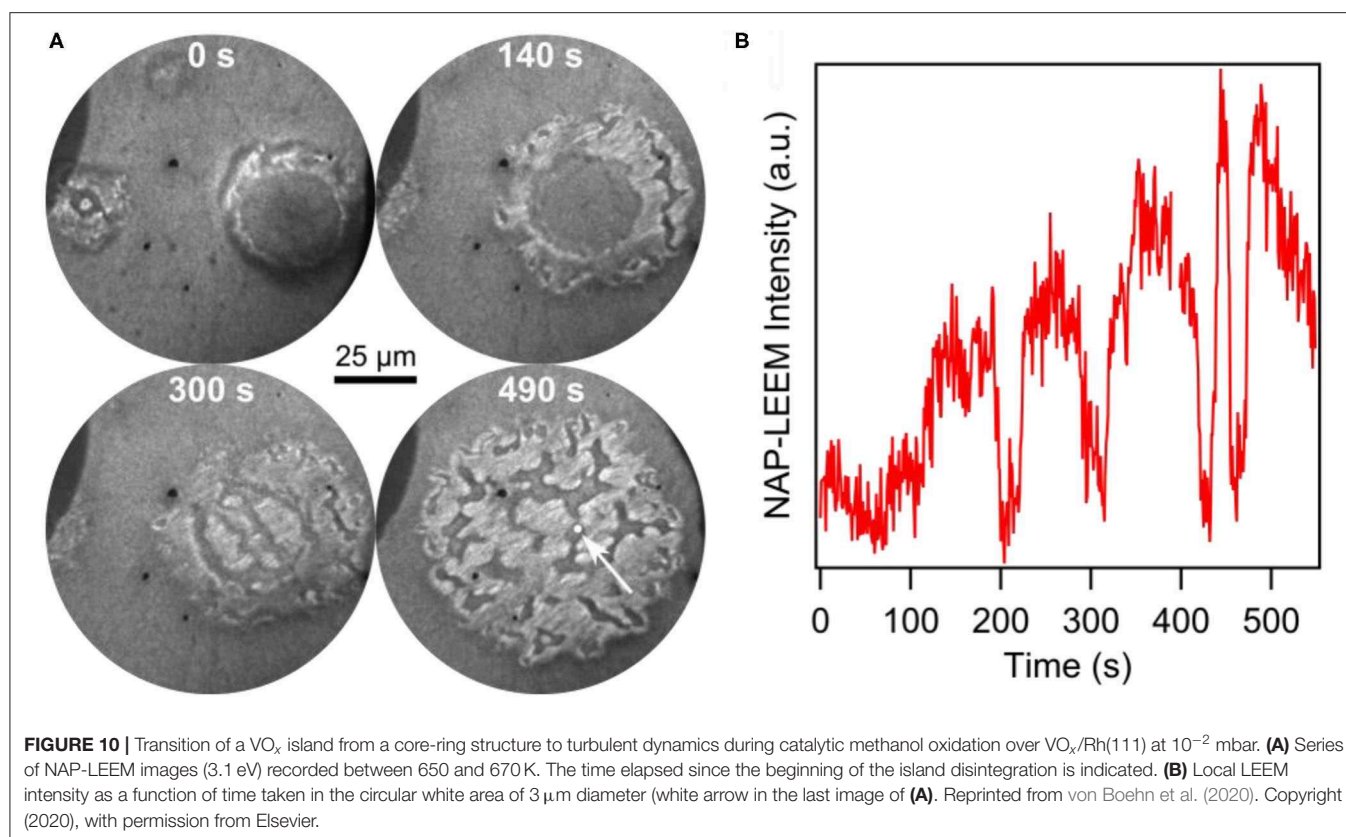
The oscillatory change of the VO_x island size requires that a mass transport of vanadium is involved in addition to the transport of oxygen. According to the Onsager relations, a gradient in the

chemical potential of oxygen is connected with a corresponding gradient in the chemical potential of vanadium (Mikhailov and Loskutov, 1991; Mikhailov, 1994). Clearly, a thermodynamic driving force for the transport of V therefore exists, but it is not clear in what form V is transported, since no experimental data exist for the diffusion inside VO_x islands. V mass transport within the island may occur via diffusion of isolated V atoms or via V-oxo complexes.

Bridging the Pressure Gap

The existence of a pressure gap in heterogeneous catalysis means that the results obtained at low pressure cannot, in general, be extrapolated to reaction conditions at higher pressure. In order to bridge the pressure gap, a variety of *in situ* and operando techniques have been developed in order to characterize a catalyst as close as possible to realistic conditions (Topsøe, 2003; Dou et al., 2017). The LEEM is a typical ultrahigh-vacuum (UHV) instrument designed for operating at 10^{-10} – 10^{-8} mbar. The operational range of LEEM has recently been extended up to 0.1 mbar, a range also denoted as near-ambient-pressure (NAP) range (Franz et al., 2019). With NAP-LEEM, the redistribution dynamics of VO_x catalysts on Rh(111) could be followed up to the 10^{-2} mbar range (von Boehn et al., 2020).

After deposition of 0.2 MLE V in vacuum, the pressure was raised into the 10^{-2} mbar range. The reaction dynamics of methanol oxidation over $\text{VO}_x/\text{Rh}(111)$ was followed with NAP-LEEM during heating up, as shown by the NAP-LEEM images in Figure 10A. Circular VO_x islands with the familiar core—ring structure form. As the temperature is raised beyond 650 K, this structure starts to disintegrate beginning at the outer ring. A slight island expansion is followed by the nucleation and growth of bright areas in the outer ring. Simultaneously, additional dark, channel-like structures develop. At slightly higher temperature, a bright phase nucleates also in the island core. After a few



seconds the original core-shell structure of the VO_x island is gone and the area is covered by bright and dark phases that continuously change. The dark, channel-like areas meander on the surface, forming long extensions, which often break and reconnect with other parts of the dark phase. A time series of the local NAP-LEEM intensity displayed in **Figure 10B** demonstrates irregular behavior. The visual impression is that of a turbulent redistribution dynamics.

Due to the lack of surface analytical techniques that can operate *in situ* in the 10⁻² mbar range, no further chemical or structural information is available. Obviously, a stable VO_x distribution on the support surface cannot be maintained in the 10⁻² mbar range, as evidenced by the turbulent redistribution dynamics. At a pressure of 10⁻² mbar, gradients in the oxygen coverage are presumably stronger than at low pressure, which might be a cause for the lack of stability in the island structure. Furthermore, in the NAP regime, the reaction conditions can no longer be considered as strictly isothermal, as it is the case under vacuum conditions up to roughly 10⁻³ mbar.

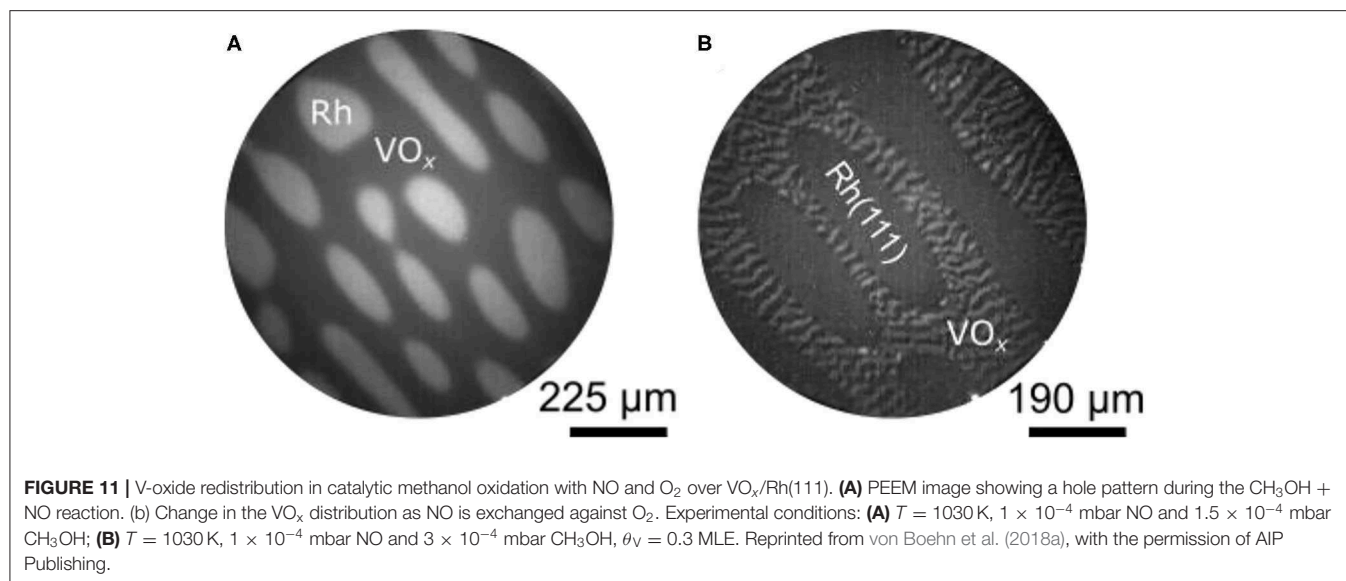
Oxidation With NO

One of the first questions that were asked after catalytic methanol oxidation exhibited quite remarkable reaction dynamics on VO_x/Rh(111), was how general the island coalescence mechanism is. Experiments in which methanol oxidation was replaced by the H₂ + O₂ reaction, the NH₃ + O₂ reaction, and catalytic CO oxidation on VO_x/Rh(111) showed in fact qualitatively the same behavior as in catalytic methanol oxidation

(von Boehn et al., 2016). However, all these reactions have in common that O₂ is used as oxidizing agent. Replacing O₂ by NO as oxygen source leads in fact to a quite different behavior (von Boehn et al., 2018a).

Figure 11A shows a PEEM image of the VO_x/Rh(111) surface after the sample has been heated up to 1030 K in a gas mixture of CH₃OH and NO. This pattern evolved from a pattern of thin parallel stripes existing around 900 K. As in methanol oxidation with O₂, the VO_x covered parts of the surface appear as dark area in PEEM, the bare Rh(111) surface as bright area. In **Figure 11A**, holes in the VO_x layer are surrounded by VO_x covered surface. With NO a pattern forms that is inverse to the island patterns seen in the oxidation of methanol with O₂. Such a hole pattern is also observed in ammonia oxidation with NO.

The VO_x hole pattern is rather static, compared to the circular VO_x islands, which move toward each other and coalesce in methanol oxidation with oxygen. Nevertheless, a coarsening of the VO_x depleted holes, similar to Ostwald ripening, is observed at 1030 K. This causes an elongation of the holes. Compared to the reaction with O₂, the interface between the VO_x covered area and the bare Rh(111) surface is broad and fuzzy. As shown with LEEM, the elongated holes are aligned to atomic steps on the Rh(111) surface (von Boehn, 2020). Atomic steps are always present on a surface resulting from a slight (unavoidable) deviation of the surface orientation from the ideal cutting angle during preparation. Another striking difference with the VO_x redistribution patterns observed with O₂ is the absence of a substructure of reduced



and oxidized phases in the VO_x layer during oxidation with NO.

The different effect that NO and O₂ have on the distribution pattern can be demonstrated nicely by exchanging the oxidizing agent NO against O₂ after a hole pattern has already been formed. The result displayed **Figure 11B** shows the same surface as **Figure 11A**, but with a gas atmosphere switched to methanol and O₂. Upon heating at 800 K a VO_x stripe pattern develops exclusively in the VO_x covered parts of the surface. As the stripes further coarsen, the familiar core—ring structure of a reduced core and an oxidized ring evolves around 900 K, and the stripe pattern is transformed into an island pattern at 1,000 K.

Compared to methanol oxidation with O₂, the oxidation of methanol with NO shows a low catalytic activity on VO_x/Rh(111). Since the dissociation rate of NO on the Rh(111) surface is rather high, one could have expected the opposite. The low catalytic activity might be the main reason why no detectable oxygen gradients exist in the VO_x layer and in the holes. The absence of a substructure in the VO_x-layer is clearly a consequence of the absence of oxygen gradients. O-concentration profiles obtained with *in situ* μXPS during the NO + NH₃ reaction showed that the interface VO_x covered surface/bare metal surface is rather broad and exhibits no steep gradient, quite in contrast to the oxidation with O₂ where gradients at the interface are steep (von Boehn, 2020). This latter observation of a broad interface can be taken as evidence for a reduced line tension at the interface compared to the oxidation reaction with O₂.

The low dynamics in the oxidation reactions with NO suggest that it is thermodynamics that is responsible for why island pattern are formed in reactions with O₂ and hole patterns in reactions with NO. More specifically, it should be a question of the interfacial energies and of the line tension. The conclusion that the line tension VO_x/metal surface is reduced in the case of NO points in this direction, but quantitative data are required in order to reach definite answers.

Summary

Ultrathin vanadium oxide layers on Rh(111) exhibit a wealth of redistribution dynamics, ranging from the development of stripe, island and hole patterns, over oscillatory behavior to turbulent redistribution dynamics under the conditions of methanol oxidation in the 10⁻⁴ and 10⁻² mbar range. Reaction-induced oxygen gradients are essential for a peculiar ripening mechanism resulting in the movement and coalescence of neighboring VO_x islands. The island movement was explained with a polymerization/depolymerisation mechanism. These oxygen gradients can also cause a phase separation inside the vanadium oxide islands, resulting in a substructure consisting of a reduced core and an outer oxidized ring. The dependence of the stability of the reduced core on the island size can lead to periodic phase transitions and simultaneous size oscillations of the vanadium oxide islands. As the total pressure is increased into the NAP regime, the core—ring structure of the VO_x islands can no longer be stabilized and turbulent redistribution is observed. Exchanging the oxidizing agent O₂ by NO results in the formation of a hole pattern instead of a VO_x island pattern. The different redistribution patterns seen with NO and O₂ are probably the consequence of the low catalytic activity of VO_x/Rh(111) in the reactions with NO, which prevents the formation of oxygen gradients.

REACTION DYNAMICS ON VO_x/RH(110)

Structure and Reactivity of VO_x/Rh(110)

Characteristic for the Rh(110) surface is its enormous structural variability as evidenced by a large number of adsorbate-induced surface reconstructions studied in detail with adsorbed atomic oxygen and nitrogen (Kiskinova, 1996). Compared to the system VO_x/Rh(111) that has been extremely well explored (Schoiswohl et al., 2004b, 2005, 2006), the main difference is that only a handful of studies have been performed for VO_x/Rh(110). It was shown that metallic vanadium on Rh(110) has a considerable

tendency to diffuse into subsurface sites forming a subsurface V/Rh alloy (Piš et al., 2013). With LEED it was demonstrated that both, V/Rh(110) and VO_x/Rh(110), exhibit a number of ordered overlayer structures upon sequential deposition, but for none of these overlayers a structure model exists (von Boehn et al., 2017). Since no structure models exist, also the V coverage calibration has to be considered as tentative.

In catalytic methanol oxidation VO_x on Rh(110) is far less reactive than on Rh(111), displaying only negligible activity with respect to formaldehyde production (von Boehn and Imbihl, 2018). Apparently, the system VO_x/Rh(110) is more complex than VO_x/Rh(111) and VO_x on the Rh(110) surface behaves quite differently than on Rh(111). Aside from a much more complex chemistry, the main new aspect that is introduced with respect to pattern formation is the anisotropy of the Rh(110) surface. A structural model of the unreconstructed Rh(110) surface in **Figure 12A** demonstrates this anisotropy.

Overview

In the following, we investigate the behavior of a submonolayer coverage of V-oxide, i. e. of a V coverage in the range $0.1 \leq \theta_V \leq 0.4$ ML, during catalytic methanol oxidation with O₂ in the 10^{-4} mbar range. The start is always a surface that after deposition of VO_x appears homogeneous in PEEM. It should be stressed that if the surface is homogeneous on a macroscopic scale ($> 1 \mu\text{m}$), on a microscopic scale it might be heterogeneous.

The sample is then heated up in a CH₃OH + O₂ atmosphere but, depending on whether we heat up above 900 K or stay below that temperature, we have a surface with VO_x islands of macroscopic size or a spatially homogeneous surface (the term homogeneous here always refers to a macroscopic length scale). Accordingly, we differentiate in the following between chemical wave patterns on a homogeneous surface and between chemical waves on a pre-patterned surface. Finally, we also consider the VO_x redistribution process itself.

Chemical Waves on a Homogeneous Surface

Traveling Interface Pulses

The CH₃OH + O₂ reaction on the unpromoted Rh(110) surface displays bistability, i. e. one has reaction fronts separating an oxygen covered surface from a surface with a low O coverage. Close to the equistability point of the two stable surface phases, one observes a phenomenon which for the first time before has been observed in catalytic ammonia oxidation on Rh(110) (Lovis and Imbihl, 2011; Rafti et al., 2015). Distortions of the interface away from its equilibrium position travel pulse-like along the interface. These traveling interface pulses (TIPs), or traveling interface modulations (TIMs) as they were called originally, represent a front instability. A general mathematical model showing their existence has been formulated (Rafti et al., 2012), but no realistic mathematical model existed at the beginning of these studies. On a surface promoted with a low coverage of V-oxide ($\theta_V = 0.1$ ML) these TIPs are much stronger in amplitude and they are much more stable than on a bare Rh(110) surface (von Boehn and Imbihl, 2017). As shown in the PEEM image in **Figure 12B**, waves with roughly triangular shape travel with a

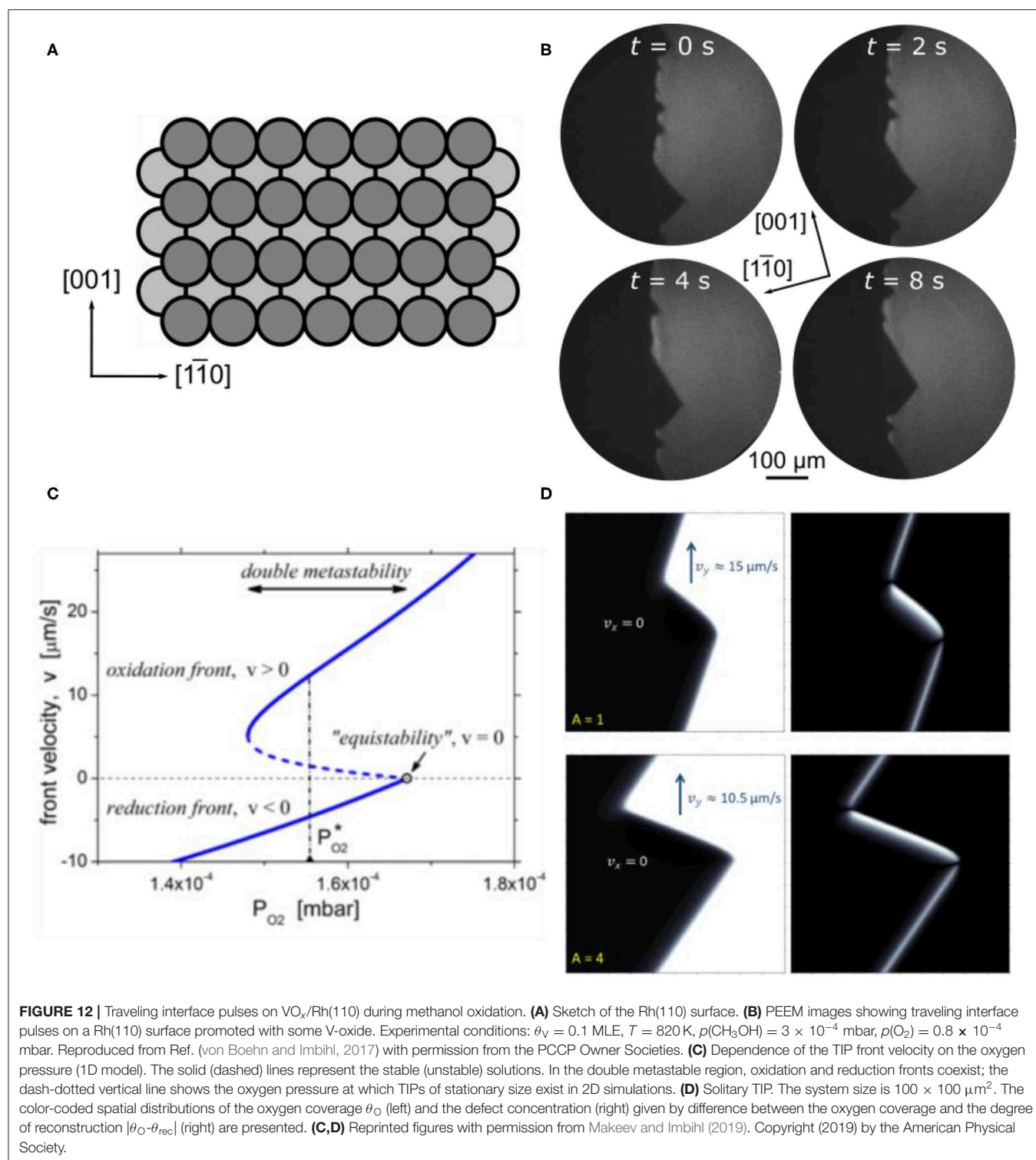
velocity of $\sim 17 \mu\text{m/s}$ along the interface. Despite the anisotropy of the Rh(110) surface no clear-cut dependence of the excitations on the crystallographic directions has been found. One notes that the area after being passed by the TIPs exhibits an enhanced brightness, which then decays within a few tens of seconds. This brightness variation indicates a temporary modification of the surface either by structural defects or by a chemical modification. Since no indication for a chemical modification was found, the brightness changes were assigned to structural defects.

To explain the formation of defects around the interface, one has to keep in mind that the interface oxygen covered/oxygen free surface also represents the boundary between two different substrate structures, the so-called “missing row” reconstructions on the oxygen covered surface and the non-reconstructed (1×1) surface of the oxygen free surface (von Boehn, 2020). Since the two substrate structures differ in their density of surface atoms, any structural variation caused, for example, by fluctuations in the oxygen coverage, will be associated with a mass transport of Rh atoms, thus causing structural defects. A roughening of the surface caused by defects will, in general, lead to an increase in catalytic activity. This means that fluctuations in the adsorbate coverages around the interface will be amplified by a positive feedback.

The mechanism sketched above is the basis of a realistic three-variable model that semi-quantitatively reproduces well the experimentally observed TIPs (Makeev and Imbihl, 2019). As shown in the bifurcation diagram of **Figure 12C**, the TIPs occur in a very narrow parameter window near the equistability point in the region of so-called dynamic bistability (or double metastability) where oxidation and reduction fronts coexist. The simulation in **Figure 12D** shows an enhanced defect concentration in the leading edge of each pulse. TIPs occur on Rh(110) during catalytic ammonia and methanol oxidation, but TIPs have not been found in the H₂ + O₂ reaction. From the proposed mechanism, one should expect that TIPs should also occur in the bistable O₂ + H₂ reaction on Rh(110). This, however, is not the case. The mathematical model provides the explanation, which is that the region of dynamic bistability becomes vanishingly small due to the fast diffusion of adsorbed hydrogen, thus removing one of the essential requirements for the occurrence of TIPs (Makeev and Imbihl, 2019).

Varying Front Geometries and Traveling Wave Fragments

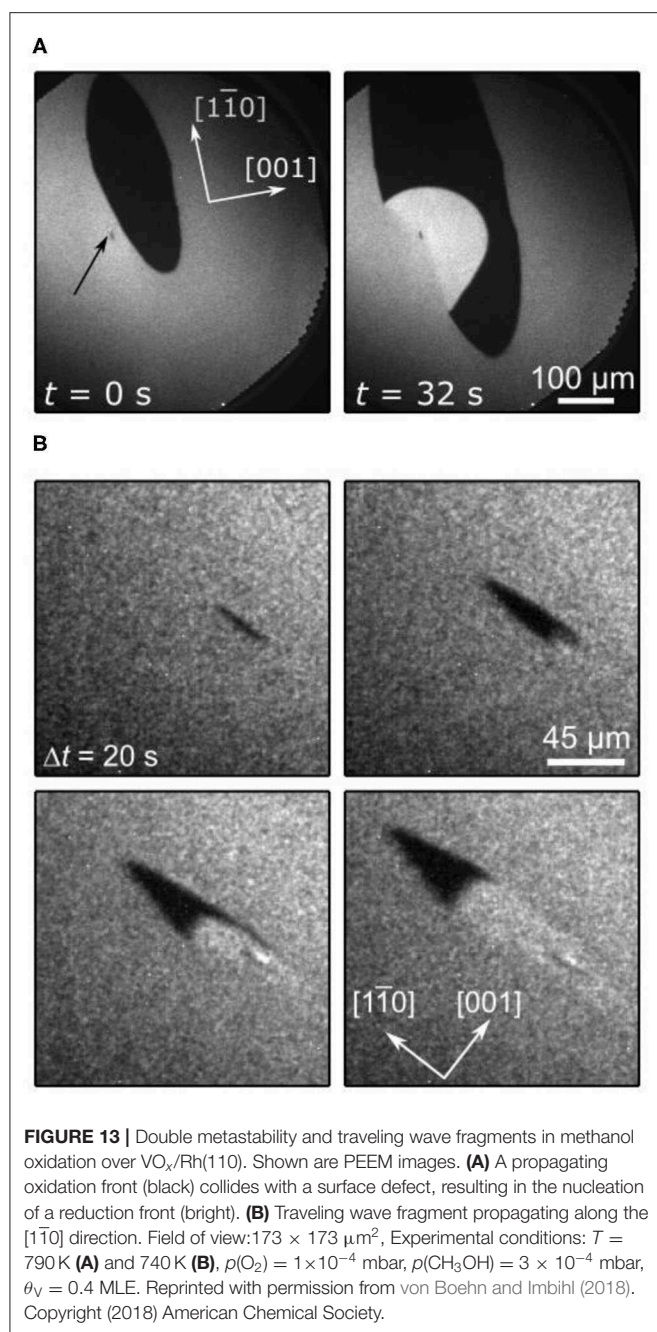
In a coverage range $0.2 \leq \theta_V \leq 0.4$, we observe dynamic bistability in a temperature range that extends roughly from 700 to 850 K. As shown in **Figure 13A**, upon a parameter change, initially an elliptical oxygen island develops imaged as dark area in PEEM. After ≈ 20 s, a bright front nucleates inside the dark island, but this bright front, as it grows, exhibits a different anisotropy than the elliptical dark island. Apparently the anisotropy of the Rh(110) surface varies depending on the type of front. Such a behavior has before been observed in the H₂ + NO reaction on Rh(110), and was traced back to a state-dependent anisotropy (Gottschalk et al., 1994; Mertens and Imbihl, 1994). In the case of the H₂ + NO reaction, the different substrate reconstructions causing the state-dependent anisotropy



have been identified, but for the present system no structure models exist yet.

Another phenomenon that results from a state-dependent anisotropy is also found here, which are traveling wave fragments (TWFs). **Figure 13B** displays PEEM images showing different stages in the development of TWFs. These TWFs typically

nucleate at some defect and then propagate with constant velocity along the $[1\bar{1}0]$ -direction, which is the direction along which the troughs of the $\text{Rh}(110)$ surface (**Figure 12A**) are oriented. TWFs have been found before in catalytic CO-oxidation on $\text{Pt}(110)$ (“soliton-like” behavior) (Rotermund et al., 1991), and in the $\text{H}_2 + \text{NO}$ reaction on $\text{Rh}(110)$ (Mertens et al., 1995).



In **Figure 13A**, and less clearly in **Figure 13B**, we can identify three distinct gray levels—a medium gray, dark and bright—which we can assign to the resting state, the excited state and the refractory state of the surface. *In situ* LEEM is feasible in the 10^{-4} mbar range. In such a LEEM/ μ LEED investigation ordered overlayers could be assigned to the different phases of chemical waves on $\text{VO}_x/\text{Rh}(110)$ (von Boehn, 2020). Even with this information a mechanistic interpretation of the patterns presented above remains very difficult due to (i) a complete lack of structure models and (ii) the missing chemical information. *In situ* μ XPS at synchrotrons requires a pressure $< 10^{-5}$ mbar,

but since the chemical waves only showed up beyond 1×10^{-4} mbar, the former condition excluded any *in situ* XPS study of chemical waves. Nevertheless, the similarity of the patterns observed here with the chemical wave patterns seen in the $\text{H}_2 + \text{NO}$ reaction on $\text{Rh}(110)$ suggests a common origin of state-dependent anisotropy, namely the switching of the surface between reconstructions with varying anisotropy.

VO_x Redistribution Patterns

Island Formation

Annealing VO_x on $\text{Rh}(110)$ in a reacting atmosphere to 1,020 K generates VO_x islands of macroscopic dimensions. Apparently, only at this temperature the mobility of VO_x on $\text{Rh}(110)$ becomes high enough to accomplish a mass transport over macroscopic distances. At 1,020 K a VO_x island size of $100 \mu\text{m}$ is reached within minutes. Similar to $\text{Rh}(111)$, the islands exhibit a substructure consisting of a dark outer ring and a bright core region in PEEM. Quite differently from $\text{VO}_x/\text{Rh}(111)$, however, the islands do not move under reaction conditions and they do not coalesce (von Boehn and Imbihl, 2018).

The VO_x islands respond to changes in the gas phase composition. Depending on whether they appear bright in PEEM ($p(\text{CH}_3\text{OH})$ high) or dark ($p(\text{CH}_3\text{OH})$ low), we speak of reduced or oxidized islands. The terms “oxidized” and “reduced” are used here on a pure phenomenological basis. In fact, the response to changes in the gas atmosphere was the main criterion to distinguish between VO_x covered areas and areas with a low VO_x coverage. Since no chemical analysis has been conducted, these assignments should best be considered as preliminary.

Chemical Wave Patterns

When, after preparation, such a surface with large reduced VO_x islands is heated up into the temperature window of dynamic bistability chemical wave patterns develop. As demonstrated by the PEEM images in **Figure 14**, TWFs nucleate and propagate across the VO_x islands. These TWFs propagate along the $[1\bar{1}0]$ -direction of $\text{Rh}(110)$, similarly to TWFs on the homogeneous surface in **Figure 13B**. Initially, dark elliptically shaped islands nucleate outside the VO_x islands. They invade the reduced VO_x islands acting as oxidation fronts. The oxidation fronts are soon followed by reduction fronts transforming the oxidized state into a refractory state appearing bright in PEEM. These bright reduction fronts also nucleate at the boundaries of the VO_x islands. The bright refractory state then relaxes into the resting state characterized by a medium gray level. A comparison with **Figure 13B** shows that the nature of the TWFs seen on the pre-patterned surface does not appear to be different from the TWFs on the homogeneous surface.

Incomplete Phase Separation

The process of VO_x redistribution could be followed *ex situ* with LEEM/ μ LEED allowing to establish correlations between the different surface phases and ordered overlayers (von Boehn et al., 2018b). The chemistry evolving in this process could not be followed *in situ* since μ XPS is not feasible at 10^{-4} mbar. However, by generating an island structure at 10^{-4} mbar in a preparation chamber followed by transfer to the LEEM chamber,

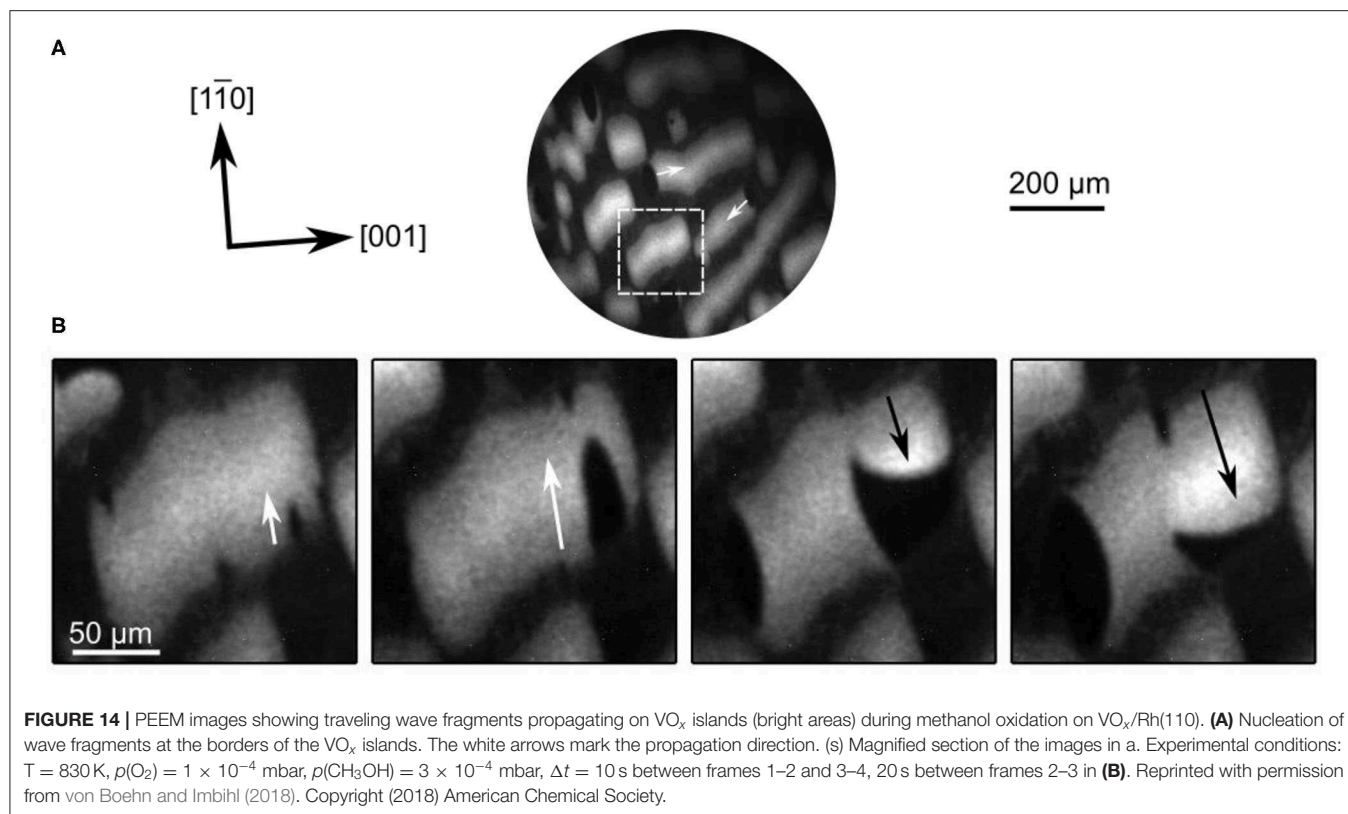


FIGURE 14 | PEEM images showing traveling wave fragments propagating on VO_x islands (bright areas) during methanol oxidation on $\text{VO}_x/\text{Rh}(110)$. **(A)** Nucleation of wave fragments at the borders of the VO_x islands. The white arrows mark the propagation direction. (s) Magnified section of the images in a. Experimental conditions: $T = 830 \text{ K}$, $p(\text{O}_2) = 1 \times 10^{-4} \text{ mbar}$, $p(\text{CH}_3\text{OH}) = 3 \times 10^{-4} \text{ mbar}$, $\Delta t = 10 \text{ s}$ between frames 1–2 and 3–4, 20 s between frames 2–3 in **(B)**. Reprinted with permission from von Boehn and Imbihl (2018). Copyright (2018) American Chemical Society.

μXPS could at least be performed *ex situ* under UHV conditions. The data showed that different from the system $\text{VO}_x/\text{Rh}(111)$ no complete phase separation into VO_x islands and into an almost VO_x free metal surface occurred. A substantial part of VO_x , roughly 15% of the signal inside the islands, is also present in the area surrounding the islands. Moreover, part of the vanadium has penetrated the Rh bulk residing in subsurface sites. These results indicate that VO_x redistribution on Rh(110) is more complex than on Rh(111).

Dendritic Growth

One starts with the uniform surface present in PEEM after deposition of 0.4 ML VO_x . Upon heating in the $\text{CH}_3\text{OH} + \text{O}_2$ atmosphere, $p(\text{CH}_3\text{OH})$ is varied such that the surface is kept in a reduced state, but not far from the transition to an oxidized state. In the temperature range 960–1020 K one observes nucleation and dendritic growth of the VO_x phase (von Boehn and Imbihl, 2018), as demonstrated by the PEEM images in **Figure 15**. Within a few minutes after the heating schedule has been stopped at 1,020 K, the whole imaged area is filled with the dendritic VO_x structure. The main axis of the dendritic structure is oriented along the $[1\bar{1}0]$ -direction, which is the direction of the $[1\bar{1}0]$ troughs of Rh(110). The dendritic growth of branches always stops short before they get in contact with each other such that they are still about 20 μm apart.

Summary

The behavior of VO_x on Rh(110) in catalytic methanol oxidation is distinctly different from VO_x on Rh(111). The catalytic activity

is much lower than on Rh(111) and we observe no moving and coalescing VO_x islands. Chemically and structurally the $\text{VO}_x/\text{Rh}(110)$ surface is much more complex than VO_x on Rh(111), since a population of subsurface sites by vanadium is involved. Furthermore, the complete lack of structural models for any of the ordered VO_x phases on Rh(110) complicates the interpretation of data. On the other hand, one is rewarded with a rich variety of intricate chemical wave patterns and VO_x redistribution processes.

Dynamic bistability with varying front geometries and traveling wave fragments can be attributed to a state-dependent anisotropy caused by surface reconstructions with different diffusional anisotropy. Despite the identification of numerous surface phases by $\mu\text{LEED}/\text{LEEM}$, an excitation mechanism for the chemical waves could not yet be established due to a lack of chemical information. *In situ* μXPS was not feasible under the conditions where chemical waves occur, a problem well known in catalysis under the name “pressure gap.” With further developments of surface analytical *in situ* techniques, capable of operating at elevated pressure, this obstacle should be overcome in the near future.

CONCLUSION

Studying catalytic reactions on $\text{VO}_x/\text{Rh}(111)$ and $\text{VO}_x/\text{Rh}(110)$, the range of non-linear phenomena in catalysis has been expanded from metal surfaces to oxidic systems. The most significant finding for $\text{VO}_x/\text{Rh}(111)$ is an island ripening

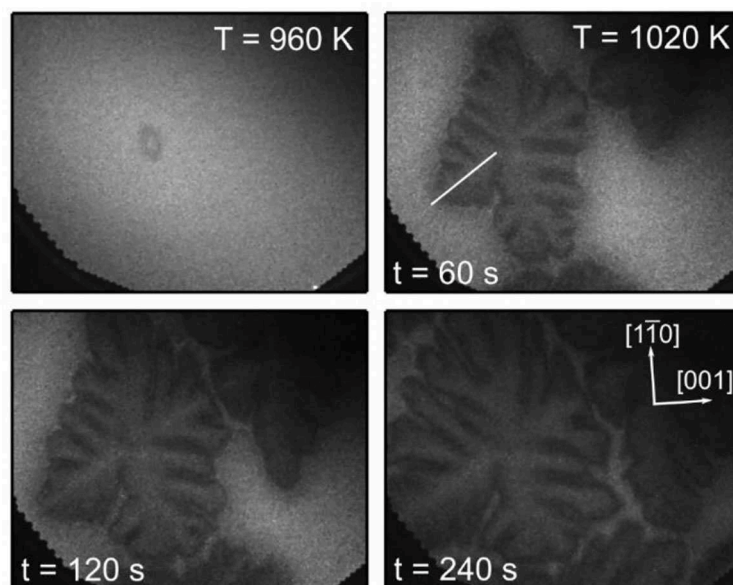


FIGURE 15 | Dendritic growth of VO_x islands on Rh(110) during methanol oxidation imaged with PEEM. Experimental conditions: $p(\text{O}_2) = 1 \times 10^{-4}$ mbar, $p(\text{CH}_3\text{OH}) \approx 3 \times 10^{-4}$ mbar, $\theta_V = 0.4$ MLE, $500 \times 400 \mu\text{m}^2$ field of view. Reprinted with permission from von Boehn and Imbihl (2018). Copyright (2018) American Chemical Society.

mechanism that operates under non-equilibrium conditions. This mechanism differs from classical Ostwald ripening and also from Smoluchowski ripening. The VO_x island coalescence could be explained with a polymerization/depolymerization mechanism. The system $\text{VO}_x/\text{Rh}(110)$ is more complex than $\text{VO}_x/\text{Rh}(111)$, but one is rewarded with a wealth of chemical wave patterns in addition to VO_x redistribution structures. Overall, one finds that supported V-oxide layers at submonolayer coverages are highly dynamic, giving rise to new phenomena that have not been observed on metal surfaces. The observations made here are closely related to the well-known “pressure and materials gap” in heterogeneous catalysis: structure and composition of the V-oxide layer are strongly pressure dependent. Moreover, comparing VO_x on Rh(111) and Rh(110), one finds that the catalytic properties and the pattern forming properties of the V-oxide layer vary drastically depending on the orientation of the metallic substrate. The results obtained here also demonstrate the relevance of non-linear effects in catalysis.

AUTHOR CONTRIBUTIONS

BB and RI wrote and edited the manuscript. All authors contributed to the article and approved the submitted version.

FUNDING

The authors are indebted to the Deutsche Forschungsgemeinschaft (DFG) for financial support through

project: 409299786. BB thanks the Department of Inorganic Chemistry of the Fritz Haber Institute of the Max Planck Society for financial support.

ACKNOWLEDGMENTS

We thank Yannick De Decker for helpful comments on the manuscript, and Andrea Locatelli and Tefvik O. Menteş for the long-lasting collaboration, which enabled to chemically characterize the systems $\text{VO}_x/\text{Rh}(111)$ and $\text{VO}_x/\text{Rh}(110)$.

SUPPLEMENTARY MATERIAL

The Supplementary Material for this article can be found online at: <https://www.frontiersin.org/articles/10.3389/fchem.2020.00707/full#supplementary-material>

Data Sheet 1 | Short description of the videos in the supplementary material.

Supplementary Video 1 | VO_x stripe and island pattern formation during methanol oxidation (PEEM).

Supplementary Video 2 | VO_x island oscillation during methanol oxidation (LEEM).

Supplementary Video 3 | Turbulent VO_x redistribution (NAP-LEEM).

Supplementary Video 4 | Formation of a VO_x hole pattern in the $\text{CH}_3\text{OH} + \text{NO}$ reaction (PEEM).

Supplementary Video 5 | Traveling interface modulations on $\text{VO}_x/\text{Rh}(110)$ during methanol oxidation (PEEM).

Supplementary Video 6 | Traveling wave fragments on VO_x islands during methanol oxidation (PEEM).

Supplementary Video 7 | Dendritic island growth on VO_x/Rh(110) during methanol oxidation (PEEM).

REFERENCES

- Barth, J. (2000). Transport of adsorbates at metal surfaces: from thermal migration to hot precursors. *Surf. Sci. Rep.* 40, 75–149. doi: 10.1016/S0167-5729(00)00002-9
- Bauer, E. (2019). “LEEM, SPLEEM and SPELEEM,” in *Springer Handbook of Microscopy*, eds P. W. Hawkes and J. C. H. Spence (Cham: Springer International Publishing), 2. doi: 10.1007/978-3-030-00069-1_9
- Boffa, A. B., Lin, C., Bell, A. T., and Somorjai, G. A. (1994). Lewis acidity as an explanation for oxide promotion of metals: implications of its importance and limits for catalytic reactions. *Catal. Lett.* 27, 243–249. doi: 10.1007/BF00813909
- Bond, G. C., and Tahir, S. F. (1991). Vanadium oxide monolayer catalysts Preparation, characterization and catalytic activity. *Appl. Catal.* 71, 1–31. doi: 10.1016/0166-9834(91)85002-D
- Carrero, C. A., Schloegl, R., Wachs, I. E., and Schomaecker, R. (2014). Critical literature review of the kinetics for the oxidative dehydrogenation of propane over well-defined supported vanadium oxide catalysts. *ACS Catal.* 4, 3357–3380. doi: 10.1021/cs5003417
- De Decker, Y., Marbach, H., Hinz, M., Günther, S., Kiskinova, M., Mikhailov, A. S., et al. (2004). Promoter-induced reactive phase separation in surface reactions. *Phys. Rev. Lett.* 92:198305. doi: 10.1103/PhysRevLett.92.198305
- De Decker, Y., Raghmy, A., and Imbihl, R. (2019). Modeling the formation and propagation of VO_x islands on Rh(111) under reactive conditions. *J. Phys. Chem. C* 123, 11602–11610. doi: 10.1021/acs.jpcc.9b00427
- Döbler, J., Pritzsche, M., and Sauer, J. (2005). Oxidation of methanol to formaldehyde on supported vanadium oxide catalysts compared to gas phase molecules. *J. Am. Chem. Soc.* 127, 10861–10868. doi: 10.1021/ja051720e
- Dou, J., Sun, Z., Opalade, A. A., Wang, N., Fu, W., and Tao, F. F. (2017). Operando chemistry of catalyst surfaces during catalysis. *Chem. Soc. Rev.* 46, 2001–2027. doi: 10.1039/C6CS00931J
- Ertl, G. (1991). Oscillatory kinetics and spatio-temporal self-organization in reactions at solid surfaces. *Science* 254, 1750–1755. doi: 10.1126/science.254.5039.1750
- Frank, B., Fortrie, R., Hess, C., Schlögl, R., and Schomäcker, R. (2009). Reoxidation dynamics of highly dispersed VO_x species supported on γ -alumina. *Appl. Catal. A Gen.* 353, 288–295. doi: 10.1016/j.apcata.2008.11.002
- Franz, A. W., Kronemayer, H., Pfeiffer, D., Pilz, R. D., Reuss, G., Disteldorf, W., et al. (2010). “Formaldehyde,” in *Ullmann's Encyclopedia of Industrial Chemistry*, ed B. Elvers (Chichester: Wiley), 1–34. doi: 10.1002/14356007.a11_619.pub2
- Franz, T., von Boehn, B., Marchetto, H., Borkenhagen, B., Lilienkamp, G., Daum, W., et al. (2019). Catalytic CO oxidation on Pt under near ambient pressure: a NAP-LEEM study. *Ultramicroscopy* 200, 73–78. doi: 10.1016/j.ultramic.2019.02.024
- Göbke, D., Romanushyn, Y., Guimond, S., Sturm, J. M., Kuhlbeck, H., Döbler, J., et al. (2009). Formaldehyde formation on vanadium oxide surfaces V₂O₃(0001) and V₂O₅(001): how does the stable methoxy intermediate form? *Angew. Chem. Int. Ed. Engl.* 48, 3695–3698. doi: 10.1002/anie.200805618
- Gottschalk, M., Eiswirth, B., and Imbihl, R. (1994). Chemical waves in media with state-dependent anisotropy. *Phys. Rev. Lett.* 73, 3483–3486. doi: 10.1103/PhysRevLett.73.3483
- Hesse, M., von Boehn, B., Locatelli, A., Sala, A., Menteş, T. O., and Imbihl, R. (2015). Island ripening via a polymerization-depolymerization mechanism. *Phys. Rev. Lett.* 115:136102. doi: 10.1103/PhysRevLett.115.136102
- Imbihl, R. (2005). Nonlinear dynamics on catalytic surfaces. *Catal. Today* 105, 206–222. doi: 10.1016/j.cattod.2005.02.045
- Imbihl, R., and Ertl, G. (1995). Oscillatory kinetics in heterogeneous catalysis. *Chem. Rev.* 95, 697–733. doi: 10.1021/cr00035a012
- Kiskinova, M. (1996). Surface structure and reactivity: reactions on face-centered cubic (110) metal surfaces involving adatom-induced reconstructions. *Chem. Rev.* 96, 1431–1448. doi: 10.1021/cr950226y
- Kropp, T., Paier, J., and Sauer, J. (2014). Support effect in oxide catalysis: methanol oxidation on vanadia/ceria. *J. Am. Chem. Soc.* 136, 14616–14625. doi: 10.1021/ja508657c
- Levin, M. (1987). The enhancement of CO hydrogenation on rhodium by TiO_x overlayers. *J. Catal.* 106, 401–409. doi: 10.1016/0021-9517(87)90252-1
- Locatelli, A., Menteş, T. O., Aballe, L., Mikhailov, A., and Kiskinova, M. (2006). Formation of regular surface-supported mesostructures with periodicity controlled by chemical reaction rate. *J. Phys. Chem. B* 110, 19108–19111. doi: 10.1021/jp065090u
- Locatelli, A., Sbraccia, C., Heun, S., Baroni, S., and Kiskinova, M. (2005). Energetically driven reorganization of a modified catalytic surface under reaction conditions. *J. Am. Chem. Soc.* 127, 2351–2357. doi: 10.1021/ja045285k
- Lovis, F., Hesse, M., Locatelli, A., Menteş, T. O., Niño, M. Á., Lilienkamp, G., et al. (2011). Self-organization of ultrathin vanadium oxide layers on a Rh(111) surface during a catalytic reaction. Part II: A LEEM and spectromicroscopy study. *J. Phys. Chem. C* 115, 19149–19157. doi: 10.1021/jp206600q
- Lovis, F., and Imbihl, R. (2011). Self-organization of ultrathin vanadium oxide layers on a Rh(111) surface during a catalytic reaction. Part I: A PEEM study. *J. Phys. Chem. C* 115, 19141–19148. doi: 10.1021/jp2065425
- Makeev, A., and Imbihl, R. (2019). Simulation of traveling interface pulses in bistable surface reactions. *Phys. Rev. E* 100:42206. doi: 10.1103/PhysRevE.100.42206
- Mavrikakis, M., Rempel, J., Greeley, J., Hansen, L. B., and Nørskov, J. K. (2002). Atomic and molecular adsorption on Rh(111). *J. Chem. Phys.* 117, 6737–6744. doi: 10.1063/1.1507104
- Menteş, T. O., Zamborlini, G., Sala, A., and Locatelli, A. (2014). Cathode lens spectromicroscopy: methodology and applications. *Beilstein J. Nanotechnol.* 5, 1873–1886. doi: 10.3762/bjnano.5.198
- Mertens, F., and Imbihl, R. (1994). Square chemical waves in the catalytic reaction NO + H₂ on a rhodium(110) surface. *Nature* 370, 124–126. doi: 10.1038/370124a0
- Mertens, G., Eiswirth, B., and Imbihl, M. (1995). Traveling-wave fragments in anisotropic excitable media. *Phys. Rev. E* 51, R5193–R5196. doi: 10.1103/PhysRevE.51.R5193
- Mikhailov, A. S. (1994). *Foundations of Synergetics I: Distributed Active Systems*. Berlin, Heidelberg: Springer. doi: 10.1007/978-3-642-78556-6
- Mikhailov, A. S., and Loskutov, A. Y. (1991). *Foundations of Synergetics II: Complex Patterns*. Berlin, Heidelberg: Springer. doi: 10.1007/978-3-642-97294-2
- Piš, I., Skála, T., Cabala, M., Šutara, F., Libra, J., Škoda, M., et al. (2012). Structural, electronic and adsorption properties of V–Rh(111) subsurface alloy. *J. Alloys Compd.* 543, 189–196. doi: 10.1016/j.jallcom.2012.07.122
- Piš, I., Stetsovych, V., Mysliveček, J., Kettner, M., Vondráček, M., Dvořák, F., et al. (2013). Atomic and electronic structure of V–Rh(110) near-surface alloy. *J. Phys. Chem. C* 117, 12679–12688. doi: 10.1021/jp402985v
- Rafti, M., Borkenhagen, B., Lilienkamp, G., Lovis, F., Smolinsky, T., and Imbihl, R. (2015). Traveling interface modulations and anisotropic front propagation in ammonia oxidation over Rh(110). *J. Chem. Phys.* 143, 184701. doi: 10.1063/1.4935274
- Rafti, M., Uecker, H., Lovis, F., Krupennikova, V., and Imbihl, R. (2012). Traveling interface modulations in the NH₃ + O₂ reaction on a Rh(110) surface. *Phys. Chem. Chem. Phys.* 14, 5260–5264. doi: 10.1039/c2cp23970a
- Rodriguez, J. A., Liu, P., Graciani, J., Senanayake, S. D., Grinter, D. C., Stacchiola, D., et al. (2016). Inverse oxide/metal catalysts in fundamental studies and practical applications: a perspective of recent developments. *J. Phys. Chem. Lett.* 7, 2627–2639. doi: 10.1021/acs.jpcclett.6b00499
- Rotermund, H. H. (1993). Investigation of dynamic processes in adsorbed layers by photoemission electron microscopy (PEEM). *Surf. Sci.* 283, 87–100. doi: 10.1016/0039-6028(93)90965-M
- Rotermund, J., and Oertzen, A., von, and Ertl, G. (1991). Solitons in a surface reaction. *Phys. Rev. Lett.* 66, 3083–3086. doi: 10.1103/PhysRevLett.66.3083
- Schlögl, R. (2015). Heterogeneous catalysis. *Angew. Chem. Int. Ed. Engl.* 54, 3465–3520. doi: 10.1002/anie.201410738

- Schmidt, T., Heun, S., Slezak, J., Diaz, J., Prince, K. C., Lilienkamp, G., et al. (1998). SPELEEM: combining LEEM and spectroscopic imaging. *Surf. Rev. Lett.* 05, 1287–1296. doi: 10.1142/S0218625X98001626
- Schoiswohl, J., Kresse, G., Surnev, S., Sock, M., Ramsey, M. G., and Netzer, F. P. (2004a). Planar vanadium oxide clusters: two-dimensional evaporation and diffusion on Rh(111). *Phys. Rev. Lett.* 92:206103. doi: 10.1103/PhysRevLett.92.206103
- Schoiswohl, J., Sock, M., Eck, S., Surnev, S., Ramsey, M. G., Netzer, F. P., et al. (2004b). Atomic-level growth study of vanadium oxide nanostructures on Rh(111). *Phys. Rev. B.* 69, 155403. doi: 10.1103/PhysRevB.69.155403
- Schoiswohl, J., Surnev, S., Netzer, F. P., and Kresse, G. (2006). Vanadium oxide nanostructures: from zero- to three-dimensional. *J. Phys. Condens. Matter* 18, R1–R14. doi: 10.1088/0953-8984/18/4/R01
- Schoiswohl, J., Surnev, S., Sock, M., Eck, S., Ramsey, M. G., Netzer, F. P., et al. (2005). Reduction of vanadium-oxide monolayer structures. *Phys. Rev. B.* 71, 165437. doi: 10.1103/PhysRevB.71.165437
- Surnev, S., Fortunelli, A., and Netzer, F. P. (2013). Structure-property relationship and chemical aspects of oxide-metal hybrid nanostructures. *Chem. Rev.* 113, 4314–4372. doi: 10.1021/cr300307n
- Thiel, P. A., Shen, M., Liu, D.-J., and Evans, J. W. (2009). Coarsening of two-dimensional nanoclusters on metal surfaces. *J. Phys. Chem. C* 113, 5047–5067. doi: 10.1021/jp8063849
- Topsøe, H. (2003). Developments in operando studies and *in situ* characterization of heterogeneous catalysts. *J. Catal.* 216, 155–164. doi: 10.1016/S0021-9517(02)00133-1
- von Boehn, B. (2020). Redistribution dynamics of ultrathin vanadium oxide layers under catalytic conditions and activation of diffusion by surface acoustic waves. (Doctoral Thesis. Hannover: Leibniz University Hannover). Available online at: doi: 10.15488/9805
- von Boehn, B., and Imbihl, R. (2017). Large amplitude excitations traveling along the interface in bistable catalytic methanol oxidation on Rh(110). *Phys. Chem. Chem. Phys.* 19, 18487–18493. doi: 10.1039/C7CP01890H
- von Boehn, B., and Imbihl, R. (2018). Chemical wave patterns and oxide redistribution during methanol oxidation on a V-oxide promoted Rh(110) surface. *J. Phys. Chem. C* 122, 12694–12703. doi: 10.1021/acs.jpcc.8b00852
- von Boehn, B., Mehrwald, S., and Imbihl, R. (2018a). Hole patterns in ultrathin vanadium oxide layers on a Rh(111) surface during catalytic oxidation reactions with NO. *Chaos* 28, 45117. doi: 10.1063/1.5020360
- von Boehn, B., Menteş, T. O., Locatelli, A., Sala, A., and Imbihl, R. (2017). Growth of vanadium and vanadium oxide on a Rh(110) surface. *J. Phys. Chem. C* 121, 19774–19785. doi: 10.1021/acs.jpcc.7b04809
- von Boehn, B., Menteş, T. O., Locatelli, A., Sala, A., and Imbihl, R. (2018b). Reactive phase separation during methanol oxidation on a V-oxide-promoted Rh(110) surface. *J. Phys. Chem. C* 122, 10482–10488. doi: 10.1021/acs.jpcc.8b02544
- von Boehn, B., Penschke, C., Li, X., Paier, J., Sauer, J., Krisponeit, J.-O., et al. (2020). Reaction dynamics of metal/oxide catalysts: methanol oxidation at vanadium oxide films on Rh(111) from UHV to 10^{-2} mbar. *J. Catal.* 385, 255–264. doi: 10.1016/j.jcat.2020.03.016
- von Boehn, B., Preiss, A., and Imbihl, R. (2016). Dynamics of ultrathin V-oxide layers on Rh(111) in catalytic oxidation of ammonia and CO. *Phys. Chem. Chem. Phys.* 18, 19713–19721. doi: 10.1039/C6CP03637F
- Wichtendahl, R., Fink, R., Kuhlbeck, H., Preikszas, D., Rose, H., Spehr, R., et al. (1998). SMART: an aberration-corrected XPEEM/LEEM with energy filter. *Surf. Rev. Lett.* 05, 1249–1256. doi: 10.1142/S0218625X98001584
- Zhang, J., and Medlin, J. W. (2018). Catalyst design using an inverse strategy: From mechanistic studies on inverted model catalysts to applications of oxide-coated metal nanoparticles. *Surf. Sci. Rep.* 73, 117–152. doi: 10.1016/j.surfrep.2018.06.002

Conflict of Interest: The authors declare that the research was conducted in the absence of any commercial or financial relationships that could be construed as a potential conflict of interest.

Copyright © 2020 von Boehn and Imbihl. This is an open-access article distributed under the terms of the Creative Commons Attribution License (CC BY). The use, distribution or reproduction in other forums is permitted, provided the original author(s) and the copyright owner(s) are credited and that the original publication in this journal is cited, in accordance with accepted academic practice. No use, distribution or reproduction is permitted which does not comply with these terms.